Techniques in Rotational Spectroscopy

Matthew Thomas Muckle
Chesapeake, Virginia

Bachelor of Science, University of Virginia, 2007

A Dissertation presented to the Graduate Faculty
of the University of Virginia in Candidacy for the Degree of
Master of Science

Department of Chemistry

University of Virginia
August, 2012

Kevin Lehmann

Eric Hudson

Timothy W. Ebbesen

Fred Richardson

Abstract

Rotational spectroscopy is a fundamental technique within basic research but implementing it in other fields such as analytical chemistry or education has been somewhat prohibitive. Thus an ambient temperature waveguide spectrometer simple and fast enough for educational use was created and tested. To extend the technique to analytical fields, a novel mm-wave chirped pulse rotational spectrometer was tested for sensitivity limits and its ability to qualitatively and quantitatively identify various molecular samples. Finally, problems with spectral purity that plague the ultimate dynamic range of broadband measurements along with potential solutions were explored. Each of these aspects represents hurdles that can be overcome to spread a remarkably powerful technique towards other disciplines.

Acknowledgements

I wish to thank first and foremost Brooks Pate for his guidance and help throughout the years. The ability to work in his lab and be at the leading edge of technology development and scientific investigation is both a pleasure and a privilege. His effort has helped mold my future scientific desire and curiosity.

I also wish to thank the members of the labs at UVA, past and present for helping me in day to day research, overall learning process and with the painful revisions of this document. Amanda, Justin, Nate, Danny, Gordon, Steve, Cristobal, Kevin, Jason, Lynn, and many others you helped inspire my drive and skill.

The many faculty at UVA who have inspired my though process and instilled me with their knowledge have my upmost appreciation.

I would like to thank my parents and family for supporting me and pushing me to always be better.

I finally wish to thank the NSF and UVA for supporting my ability to research novel and exciting science during my time at UVA.

Table of Contents

Chapter I:

Extending Rotational Spectroscopy

Rotational spectroscopy has been a main stay throughout the last century for extremely accurate structure determinations of gas phase molecules[1-3], weakly bound clusters[4-6], electronic properties (i.e. dipole moments)[11,12], and most recently, reaction and isomerization dynamics[7,8] Its ability to accurately determine structures via the rotational spectrum and isotopic substitution leaves it as one of the most powerful fingerprinting techniques available. Yet despite its prowess in the physical field rotational spectroscopy has yet to be successfully incorporated as an analytical technique in industry or education. The types of rotational spectroscopy widely in use (Stark modulated[11], Fabry Perot cavity[17], long pass absorption[16], and chirped pulse pulsed jet[19]), while powerful in certain aspects, all have limiting factors. In order to understand how to push this sensitive technique beyond the pure research sphere one should first consider a rough overview of the operations of each technique and the physical processes leading to the rotational spectrum.

Rotational Spectra

Rotational spectra take advantage of transitions using the rotational degrees of freedom of molecules and clusters. For any three dimensional molecule an axis system

can be defined (principal axis system) where the origin is at the center of mass and the inertial tensor (Eq. 1) is purely diagonal[9]. These diagonal elements are then known as the principal moments of inertia. The principal moments are then used to derive the rotational constants as shown in Eq. 2.

$$I = \begin{bmatrix} I_{AA} & I_{AB} & I_{AC} \\ I_{BA} & I_{BB} & I_{BC} \\ I_{CA} & I_{CB} & I_{CC} \end{bmatrix} = \begin{bmatrix} \sum m(y^2 + z^2) & -\sum m(x * y) & -\sum m(x * z) \\ -\sum m(y * x) & \sum m(x^2 + z^2) & -\sum m(y * z) \\ -\sum m(z * x) & -\sum m(z * y) & \sum m(x^2 + y^2) \end{bmatrix}$$

$$I = \begin{bmatrix} I_A & 0 & 0 \\ 0 & I_B & 0 \\ 0 & 0 & I_C \end{bmatrix} \quad \textbf{Eq.1}$$

$$I_B = \frac{\boldsymbol{h}}{8 * \pi * c * B} \quad \textbf{Eq.2}$$

The rotational constants are the primary source of information used to derive the rotational energy levels of the molecule via the rotational Hamiltonian. Selection rules limit the total number of transitions between states and drive the frequencies of the final spectrum. Relative line intensities are then determined by the overlap integral of the two states with the dipole operator μ (Eq. 3)(which is also responsible for the aforementioned selection rules), the population of the level given by the Boltzmann Population distribution function, and the degeneracy of the level.

$$< \boldsymbol{J_{KK}} | \mu | \boldsymbol{J'_{K'K'}} > \quad \textbf{Eq. 3}$$

$$\boldsymbol{Q} = \sum_{\boldsymbol{i}} \boldsymbol{g_i} * \boldsymbol{e}^{-\frac{\boldsymbol{E_i}}{\boldsymbol{k} * \boldsymbol{T}}} \quad \textbf{Eq. 4}$$

This degeneracy and Boltzmann populations become important when choosing a final frequency range in which to run an experiment. The total number density of molecules to volume ratio will remain constant with a change in temperature in a closed cell but the total density of lines will increase with temperature. The number of lines is a function of the total number of energy states that are thermally populated known as the partition function, Q (Eq. 4), where g is the degeneracy of the i^{th} state, E is the energy of the i^{th} state, k is the Boltzmann constant, and T is the temperature. The resulting number of states will increase roughly as $T^{3/2}$ (for an asymmetric molecule, $T^{1/2}$ per rotational degree of freedom) greatly increasing the complexity of the spectrum while reducing the maximum intensity of the spectrum as the total population is divided between more states (Figure 1). Thus as the thermal energy increases the higher energy states (with higher *m* degeneracy) become more and more populated, shifting the peak intensity to higher frequencies.

Structure analysis and molecular identification

Because the rotational constants that determine the frequencies of the transitions in the spectrum are determined by the mass distribution of the molecule in question, small changes in mass (as small as the addition of a single

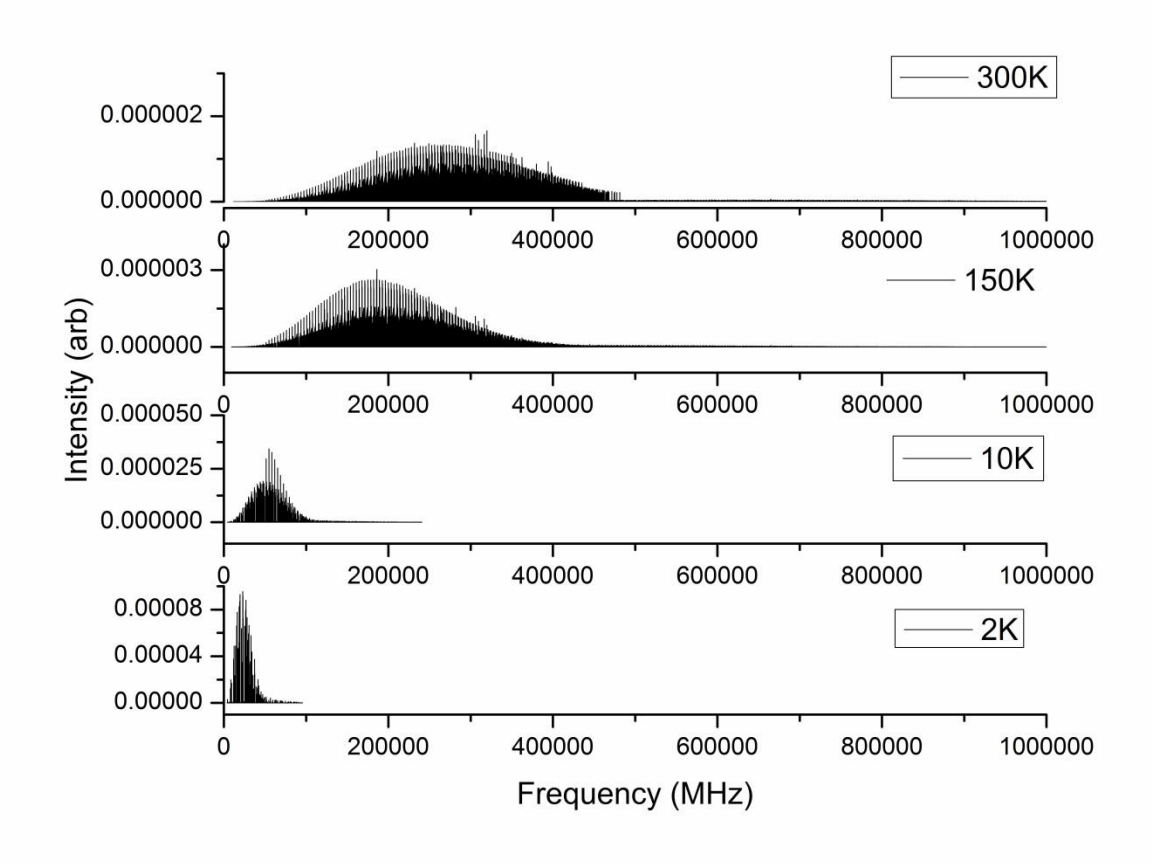

Figure 1: Simulated spectra of Flurobenzene at 2,10, 150, and 300K showing the shift in intensity to higher frequency and drop in peak intensity with higher temperature. Simulations were performed with SPCAT.

hydrogen) will change the resulting spectrum. Since most normal molecular species must abide by chemical bonding rules and steric interactions, the chances of having two systems with exactly the same rotational constants is very near zero. This structural sensitivity coupled to the high experimental resolution of the technique (2MHz- 5 KHz typical) makes rotational spectroscopy a highly accurate and sensitive fingerprinting technique. Molecular identification can be made by comparison to *ab intio* calculations or by structure analysis through isotopic substitution.

The ability to directly determine structure experimentally through isotopic substitution is a feature that is unique to microwave spectroscopy and provides a vast increase in the certainty of assignment since no assumptions (other than simple chemical rules such as atoms cannot overlap) about the molecule's identity are needed to derive its structure. Small mass changes from individual substitutions of isotopes will create a new spectrum slightly shifted from its normal species (Figure 2). If these spectra are recorded in natural abundance then their intensities will be scaled from their normal species by a ratio equal to their natural abundance, which greatly aids in locating the new spectral lines. Because the energy of the chemical bonds does not change with isotopic substitution (apart from zero point shifts which are mostly negligible beyond Hydrogen), the structure of the isotopolog will be nearly identical to that of the normal species apart from a shift in the center of mass. Thus by using Kraitchman's equations[10] the distance of that atom from the center of mass can be calculated by the shift in the molecule's moment of inertia. This can be repeated for all atoms, that have multiple stable isotopes, in the system to obtain a full molecular structure, often with sub-angstrom accuracy[1-3].

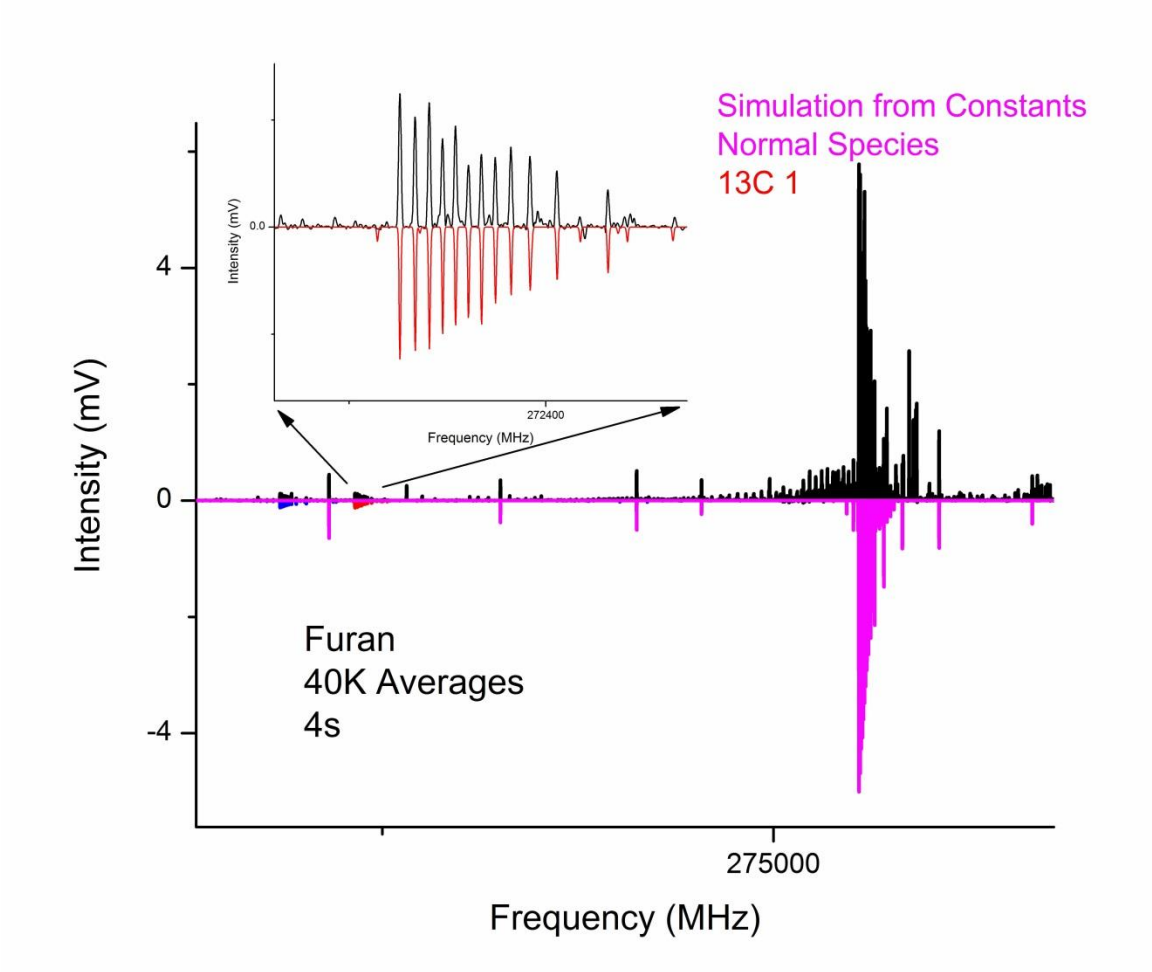

Figure 2: Experimental spectrum of Furan (black, positive) with simulations of its normal species (maroon, negative) and a carbon 13 isotopomer (red, negative) showing the shift in the spectrum with isotopic substitution.

Stark modulated flow cell and Long pass absorption

The stark modulated waveguide spectrometer[11] was the workhorse of the field up until the gradual transition into the use of the Fabry-Perot cavity in the 1970's, though some are still in use today for specific applications. Here a microwave waveguide was sealed to vacuum where sample gas could be introduced primarily as a flowing cell. A single frequency source was modulated around a small frequency range while a stark field was applied to waveguide. As the oscillator swept through a molecular transition, the detector on the opposite end of the waveguide recorded modulation in the transmitted power to produce a final spectrum.

Using a cell in this manner forced measurements to be run at or near room temperature, which, as discussed previously, is not the most sensitive method due to the scaling of the partition function and typical high frequency Boltzmann peak. On a positive note the technique allowed one to extract very accurate diploes via the Stark effect.[12] Additionally, the systems ran in narrow instantaneous bandwidths (single frequency oscillator) leading to long measurement times. Similarly, unlike future emission techniques, the cells ran in absorption and the measurement therefore was not background free . The stark modulation technique was reasonably sensitive; Nigh *et.al.*[14] reports ppm level detection on ammonia. This sensitivity level was dependent on the voltage breakdown of the stark plates combined with the gain applied to the crystal detector. The stark modulated cell was actually built and sold as a commercial

instrument by Hewlet Packard as the MRR Spectrometer in the late 1960s and early 1970's but was not successfully incorporated outside of academic research.

The long pass absorption spectrometer runs very similarly to the Stark modulated system[15,16]. Instead of modulating the spectrum with a stark field the frequency source is modulated and scanned to produce an absorption measurement at the detector. The technique is often only used for higher frequency spectra (THz/mm-wave).

Fabry Perot

The second technique was the Fabry Perot spectrometer developed by Balle and Flygare [17]. This spectrometer was typically designed to work between 4-40GHz similar to the original lower frequency ranges of the stark modulated instrument. Yet it had the advantage of cooling the spectra down to rotational temperatures in the range of ~2K. Low rotational temperature is highly advantageous as it significantly reduces the partition function as well as causing the Boltzmann intensity peak to shift within the measurement bandwidth. This greatly enhanced the overall sensitivity of the system.

Unlike adsorption measurements the Balle-Flygare type instrument measured molecular transitions via emission, which allowed the measurement to be performed background free. The Fabry-Perot cavity allowed for passive amplification of the polarizing pulse and molecular emission enabling the instrument to run at low powers and greatly enhancing the sensitivity as compared to single pass background instruments. Additionally, by using a coaxial nozzle arrangement[18], the instrument could achieve

linewidths on the level of a few KHz (FW-HM), making the determination of line centers and molecular constants extremely precise as well.

However, because of the small bandwidth and long measurement times for high sensitivity full band measurements it has been difficult to extend this spectrometer outside the research field. Scanning measurements over long times can cause the sample to degrade over time or even cause sample conditions to change partway through the spectrum leading to uncertainty in the final sample composition. Furthermore, the spectrometer is often run to equalize population between levels which takes the pulse outside the weak pulse limit and can lead to uncertain relative intensities if not all transitions are fully polarized. This removes the ability to accurately and quantifiably determine the abundance of the measured species.

Broadband Chirped Pulse FTMW:

Chirped pulse pulsed jet spectroscopy, developed at the turn of the millennium by Brown *et. al.*[19] , built off the enhanced cooling effects of a supersonic pulsed jet used in the Balle-Flygare instrument but took advantage of improvements in digital electronics to greatly increase the bandwidth per unit time of the final measurement. The instrument was able to measure 12GHz (6.5-18.5GHz) of bandwidth in a single nozzle acquisition as compared to the <1MHz of the Balle-Flygare instrument at the cost of single acquisition sensitivity. Recent improvements with multi free induction decay (FID) collection and multiple nozzles have greatly increased the sensitivity of chirped pulse spectroscopy allowing for the measurement of extremely weak and unstable species in relatively short

measurement times[4]. The chirped pulse technique also allows for a flat polarizing pulse, which gives the final spectrum extremely accurate and reliable relative intensities as demonstrated by Brown *et al* with isotopic measurements of OCS.

This instrument with its sensitivity, speed, and ability to measure relative abundances makes some of the largest steps towards creating a viable instrument to extend beyond the realm of basic research. With enhanced software techniques the limiting factors of spectral analysis can be minimized but the instrument is still extremely large (currently the size of a medium truck, though it can be compacted significantly) with significant power requirements and would thus need a specialized environment to be run and used. Multiple remedies have been implemented to reduce the total size of the instrument by increasing its frequency range and moving to ambient temperature cells

Choosing the Design

Finally one has to choose how to build and apply the next generation spectrometer that can hopefully pass beyond staying only in high end research and into analytics and education. Integrating a research quality rotational instrument into teaching labs at universities would aid greatly into both understanding modern instrumentation and learning quantized energy systems. Some compromises must made among available technology, cost, ease of use, and sensitivity. Low frequency spectrometers will tend to be far less expensive, but at 300K sensitivity may suffer even with the polarization powers available. High frequency instruments will be highly sensitive but costly and

often only have low excitation powers. Yet, both applying the broadband techniques and the ease of use of the ambient temperature systems provide a strong baseline for usability and sensitivity that are needed to help extend microwave techniques. Thus an ambient temperature low frequency (8-18GHz) chirped pulse microwave spectrometer for educational use will be presented, along with applications of analytical techniques to the high sensitivity of a high frequency (260-295GHz) instrument. Finally, complications with spectral purity of these broadband systems and their pulsed jet counterparts will be introduced and potential solutions presented.

References

[1]Shipman, S.T., Neil, J.L., Suenram, R.D., Muckle, M.T., Pate, B.H., 2011. Structure Determination of Strawberry Aldehyde by Broadband Microwave Spectroscopy: Conformational Stabilization by Dispersive Interactions. J. Phys. Chem. Lett. 2, 443–448.

[2]Steber, A.L., Neill, J.L., Zaleski, D.P., Pate, B.H., Lesarri, A., Bird, R.G., Vaquero-Vara, V., Pratt, D.W., 2011. Structural studies of biomolecules in the gas phase by chirped-pulse Fourier transform microwave spectroscopy. Faraday Discuss. 150, 227–242.

[3]Bak, B., Christensen, D., Dixon, W.B., Hansen-Nygaard, L., Andersen, J.R., Schottländer, M., 1962. The complete structure of furan. Journal of Molecular Spectroscopy 9, 124 – 129.

[4]Perez, C., Muckle, M.T., Zaleski, D.P., Seifert, N.A., Temelso, B., Shields, G.C., Kisiel, Z., Pate, B.H., 2012. Structures of Cage, Prism, and Book Isomers of Water Hexamer from Broadband Rotational Spectroscopy. Science 336, 897–901.

[5]Xu, Y., Jaeger, W., 2008. Isotopic studies of the binary complex He-OCS. J. Mol. Spectrosc. 251, 326–329.

[6] Daly, A.M., Douglass, K.O., Sarkozy, L.C., Neill, J.L., Muckle, M.T., Zaleski, D.P., Pate, B.H., Kukolich, S.G., 2011. Microwave measurements of proton tunneling and structural parameters for the propiolic acid–formic acid dimer. The Journal of Chemical Physics 135, 154304–154304–12.

[7]Dian, B.C., Brown, G.G., Douglass, K.O., Pate, B.H., 2008. Measuring picosecond isomerization kinetics via broadband microwave spectroscopy. Science 320, 924–928.

[8] Neill, J.L., Muckle, M.T., Zaleski, D.P., Steber, A.L., Pate, B.H., Lattanzi, V., Spezzano, S., McCarthy, M.C., Remijan, A.J., 2012. Laboratory and tentative interstellar detection of trans-methyl formate using the publicly available Green Bank Telescope PRIMOS survey. arXiv:1206.6021.

[9]Gordy, W., Cook, R., 1984. Microwave Molecular Spectra, (3rd ed). Knovel.

[10]Kraitchman, J., 1953. Determination of Molecular Structure from Microwave Spectroscopic Data. American Journal of Physics 21, 17.

[11]McAFEE, K.B.J., HUGHES, R.H., WILSON, E.B.J., 1949. A Stark-effect microwave spectrograph of high sensitivity. The Review of scientific instruments 20.

[12] Blanco, S., Lopez, J.C., Lesarri, A., Alonso, J.L., Kleiner, I., 2001. The microwave spectrum of pentafluoroethane. J. Mol. Struct. 599, 219–223.

[14]NIGH, F., BRODWIN, M., 1978. MINIMUM DETECTABLE POLLUTANT CONCENTRATIONS WITH STARK MODULATED MICROWAVE SPECTROSCOPY. IEEE Trans. Instrum. Meas. 27, 89–93.

[15]Winnewisser, G., Krupnov, A.., Tretyakov, M., Liedtke, M., Lewen, F., Saleck, A., Schieder, R., Shkaev, A., Volokhov, S., 1994. Precision broadband Spectroscopy in the Terahertz Region. Journal of Molecular Spectroscopy 165, 294–300.

[16]Ziurys, L.M., Barclay, W.L., Anderson, M.A., Fletcher, D.A., Lamb, J.W., 1994. A millimeter/submillimeter spectrometer for high resolution studies of transient molecules. Review of Scientific Instruments 65, 1517–1522.

[17]BALLE, T., FLYGARE, W., 1981. FABRY-PEROT CAVITY PULSED FOURIER-TRANSFORM MICROWAVE SPECTROMETER WITH A PULSED NOZZLE PARTICLE SOURCE. Rev. Sci. Instrum. 52, 33–45.

[18]Grabow, J., Palmer, E., McCarthy, M., Thaddeus, P., 2005. Supersonic-jet cryogenic-resonator coaxially oriented beam-resonator arrangement Fourier transform microwave spectrometer. Rev. Sci. Instrum. 76.

[19]Brown, G.G., Dian, B.C., Douglass, K.O., Geyer, S.M., Shipman, S.T., Pate, B.H., 2008. A broadband Fourier transform microwave spectrometer based on chirped pulse excitation. Rev. Sci. Instrum. 79.

Chapter II:

Ambient Temperature Waveguide Spectrometer

Rotational and microwave techniques have evolved over the years where each technique has brought new advantages, but rarely have they rendered each other obsolete. Stark Modulated absorption flow cells[1,2], Fabry-Perot cavity FTMW[2,3], and Chirped Pulse FTMW[3,4] all still work together in their specified roles. As previously discussed in chapter I, each of these instruments are incredibly powerful research tools, but they are difficult to implement in the classroom either because of high construction and upkeep costs or long measurement times due to narrow bandwidth when trying to observe full broadband spectra. However, the question arises can one take the abilities from each of these instruments and create a low cost instrument capable of both modern research and providing an affordable educational tool? The key is molding advantages that were learned from each incarnation of these instruments into one while trading off as little as possible and keeping the instrument low cost.

One potential way to do this is to take the chirped pulse for large bandwidths and use it in a waveguide cell working at room temperature and low frequency. The larger bandwidths, with no moving parts, reduces the overall measurement time, allowing for a

measurement to fit smaller timespans available to students. Another advantage of using the chirped pulse is an instantaneously visual spectrum is collected, rather than a single transition during a single acquisition. For many students this is a concept that relates better with similar common instruments in the classroom (FTIR, NMR, UV-VIS). The drawback is that ultimate sensitivity will be lost because of the increased partition function and Boltzman peak shift relative to the 2K measurements in a pulsed jet. Yet, the removal of the large vacuum chambers and pumping systems from the supersonic jet instruments greatly lowers the cost, size and complexity of the experiment, allowing it to be utilized in the classroom. By continuing to work as a Fourier transform emission spectrometer, modulation methods, like the Stark cell uses, do not have to be used which further removes the need for high voltage equipment.

Commercial microwave frequency techniques such as radar and communication make components in the range of 6-18GHz highly available for low cost which make an ideal target for creating a cost efficient educational spectrometer. Though not ideal in terms of the Boltzmann population distribution (Figure 1) at 300K, the former use of stark modulated spectroscopy in this region show it is indeed possible for a select group of small molecules. The added

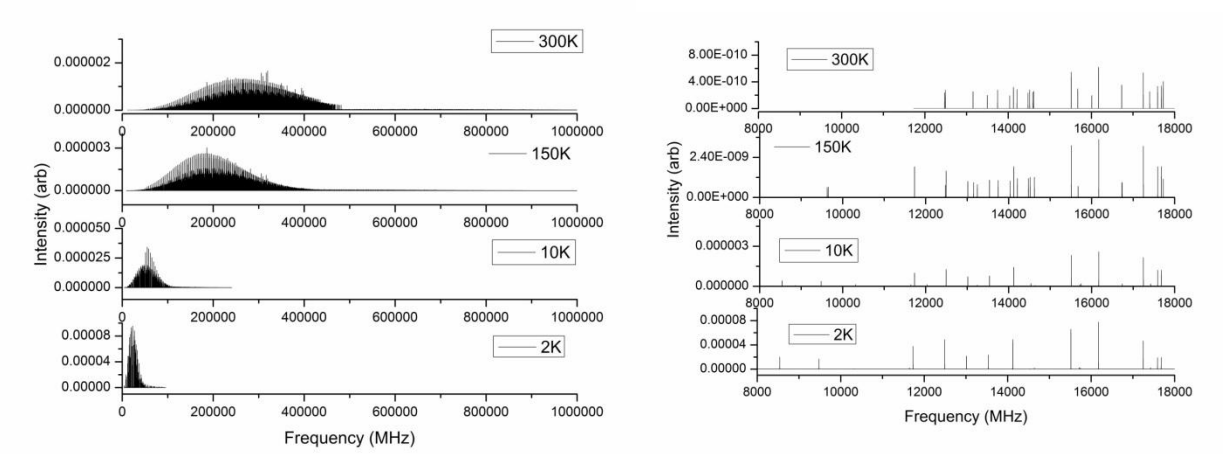

Figure 1: Simulated spectra at various temperatures for a large rigid molecule, Flurobenzene. At room temperature(top) little intensity exists in the spectral region from 8-18GHz. The ideal intensity region appears around 300GHz.

benefit of the coherently detected background free FTMW detection gives added sensitivity, which allows for detection of weaker species.

The total cost of the entire instrument created was <$40,000USD where large portions could still be saved with lower cost digitizers and waveform generators. Estimations after cost reduction place a final instrument construction cost at near $20,000USD or less. A schematic of the final instrument and components can be found in Figure 2.

Sample Cell

A gas cell was prepared using a 2-ft section of double ridge waveguide (WRD-750) operational between 6-18GHz. Longer lengths can be used for increased signal, but the above length was selected to fit neatly in a secondary vacuum chamber for long average experiments to lower leak rates. The system was sealed to vacuum at either end of the waveguide by gluing two mica sheets (<1mm thickness) over the open ends. A pressure section was attached in the middle allowing access for sample introduction by a small 1/8" NPT connector. The system was capped with two SMA to waveguide adaptors to allow the introduction and detection of the microwave radiation.

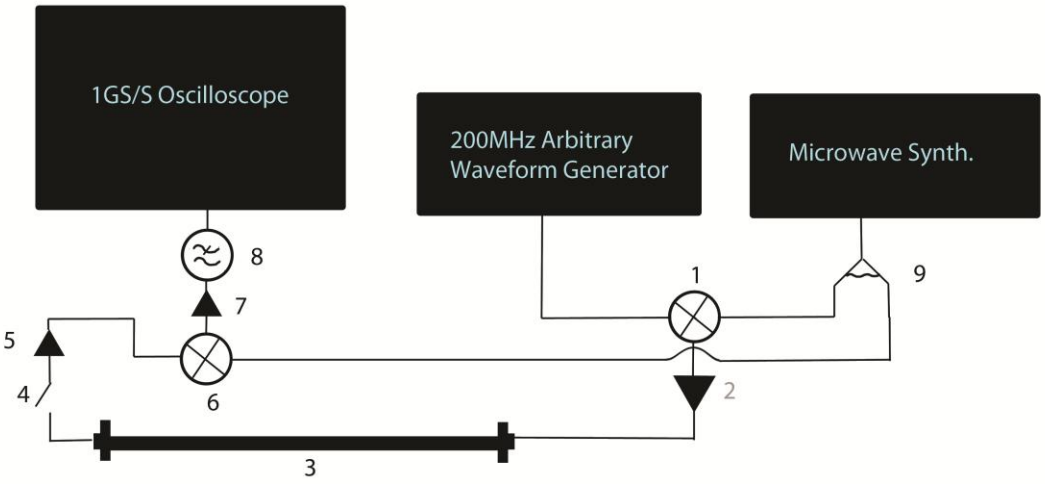

Figure 2: Schematic of the ambient temperature waveguide spectrometer 1. Single sideband upconverter 2. 1W 6-18GHz amplifier 3. Waveguide gas cell 4. PIN diode protection switch 5. 40db gain detection amplifier 6. Image rejection mixer 7. DC-1GHz amplifier 8. 1GHz Low pass filter

Excitation

A 240MHz chirped pulse (DC-240MHz) with a typical length of 250 ns was generated by an arbitrary function generator and up-converted to 6-18 GHz by mixing with a local oscillator produced by a tunable microwave synthesizer via a single sideband modulator. This single sideband modulator attenuates the production of the upper sideband from the output by 20dB, allowing for the full power of the excitation to be used in the desired range. This chirped pulse was amplified in a 1W TTL controlled solid state amplifier and introduced into the gas cell via the waveguide to SMA adaptor.

Detection

After a small time delay of less than 1μs (to allow any ringing effects of the excitation pulse to die down) a fast PIN diode switch on the detection end opened via TTL control. This switch was in place to protect the detection amplifier from oversaturation due to the power of the excitation pulse. The molecular emission signal, known as the free induction decay(FID), was then collected for a time period of 2 to 4μs and amplified by 40dB by a general purpose amplifier. A general purpose amplifier was chosen over low noise options to save a significant fraction of cost (>$1000USD). After amplification, the signal was sent to an image rejection mixer and downconverted to DC-240MHz. The combination of an image rejection mixer (down converting single side band mixer) and single sideband modulator allows for less convoluted spectra. Without removing the second sideband the digitized spectrum would be a superposition of signal from both sidebands and aliased signals from the down conversion. These single

sideband components are not necessary but greatly reduce the complexity of the final signal, allowing for greater ease when teaching students. Finally, the downconverted signal was passed through a low cost 20dB IF amplifier to reduce bit noise, followed by a 1500MHz low pass filter to remove aliased signals and noise, and finally digitized on a 500MHz hardware bandwidth 5GS/S Tektronix oscilloscope running at 2.5GS/S. The local oscillator was tuned in steps of 200MHz to cover the full band in the range of 7-18GHz.

Dynamic range and sensitivity

To demonstrate the dynamic range and sensitivity of the instrument ammonia was used. The inversion motion of ammonia[7] provides a somewhat complicated spectrum, as opposed to a rigid rotor, but it is very useful as a teaching tool for student labs on measuring tunneling rates and barriers[8,9]. Fortunately the tunneling motion makes it so some reasonably intense lines appear within the operating bandwidth of the instrument. This allows for a strong demonstration of the potential dynamic range one can measure as well for use with isotopic measurements and effects.

The sample cell was dosed with 10mtorr of ammonia gas where no additional purification was performed. The rotational spectrum between 9.8 and 18.2GHz was recorded in 200MHz intervals with 1 million averages per segment (15min/segment). The signal was recorded at 2.5GS with a 4 microsecond window. A Kaiser Bessel window was applied to improve baseline line width, and the signal was zero padded by a factor of 4 in length to smooth line shapes in the Fourier transform. The full resulting

spectrum is shown in Figure 3 compared to a simulated spectrum of published lines from Jet Propulsion Laboratory (JPL)[10]. Additionally Figure 3 shows inserts of experimental lines of $^{15}NH_3$ (0.36%) and NH_2D (0.045%) in natural abundance yielding a dynamic range of ~3000:1.

Relative intensities

The second test is looking at relative intensities across the entire band. Ideally, to keep pace with the current broadband systems in existence, the spectrometer should exhibit a flat intensity profile across its full bandwidth. To do this, methyl formate was chosen for its high line density at room temperature at these frequencies. When in the weak pulse limit, the signals should scale linearly with the incident electric field while having intensities proportional to the square of the transition moment. One possible deviation from the predicted relative intensities would be transition moments being strong enough to deviate from the linear portion of the weak pulse limit. Pulse lengths and pulse attenuation were adjusted experimentally to optimize the signal without saturating any transitions to avoid this problem.

A second source of non-linearity in gain, could be from the response curves of components. Mixers and amplifiers typically will exhibit a non-flat gain factor across a large bandwidth. Fortunately this can be accounted for with gain correction curves if the problem is significant.

For this demonstration, the sample cell was dosed with 8mtorr of methyl formate evaporated from a liquid sample from Sigma Aldrich. Residual high

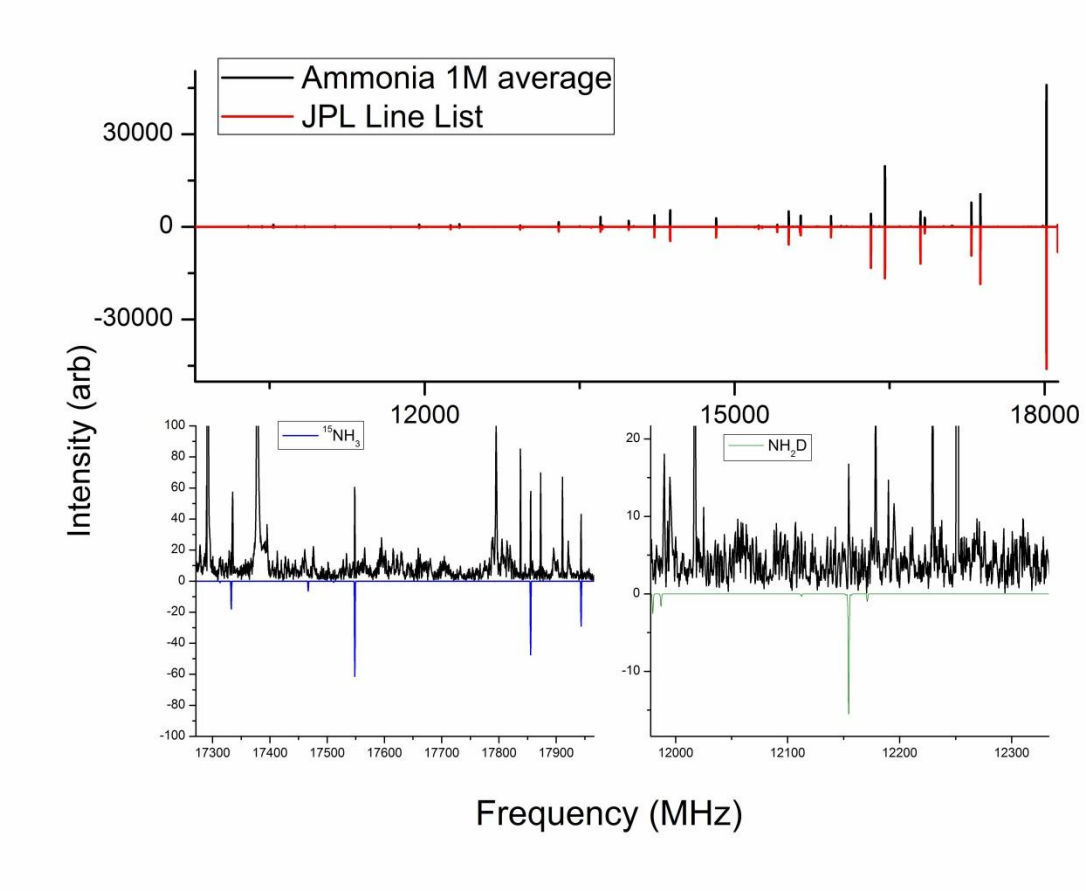

Figure 3: Experimental spectrum of Ammonia (NH_3) at 300K (black, postive) plotted against the a simulated spectrum from a JPL catalog line list (red, blue green, negative). Selected transitions from the ^{15}N and single deuterium isotopolog spectra are shown in the bottom insets.

vapor pressure contaminates were removed with a single freeze, pump, thaw purification. The rotational spectrum between 9.8 and 18.2GHz was recorded in 200MHz intervals with 1 million averages per segment. The signal was recorded at 2.5GS with a 4 microsecond window. A Kaiser Bessel window was applied to improve baseline line width and the signal was then zero padded by a factor of 4.

The resulting set of 200MHz sections were stitched together and plotted against a simulated spectrum from the JPL line catalog[10]. The JPL spectrum was scaled to match the experimental intensity in Figure 4 for methyl formate. The majority of unmatched lines are assumed to be primarily due to low lying vibrationally excited states of methyl formate. Small low vapor pressure impurities are also possible, but the major high vapor pressure impurities were removed with the freeze pump thaw purification. No attempt to fit these spectra was made.

On visual comparison it would appear that the overall intensity relationship between the two spectra was remarkably consistent. A few of the lines appear to regularly show lower than expected experimental intensity. This hints to a non-flat gain curve in a component, most likely from the image rejection mixer. These gain effects can be accounted for and normalized, but since their effects happen before the digitizer the noise of the spectrum would be increased as well. Thus no correction was performed for a smooth baseline at the cost of decreased intensity accuracy. The gain correction however could be applied to the simulated spectrum to preserve a flat baseline in the experimental, but this method was not performed.

Conclusion

Using a chirped pulse waveguide as a source for an educational level spectrometer still capable of novel research is a relatively effective and inexpensive solution. The instrument performs with high enough sensitivity to reach isotopomer measurements in the time period of a typical lab period. Additionally, the spectrometer is able to measure large bandwidths at good relative intensities yielding a visually appealing and interpretable spectrum suitable to introductory instruction.

Due to its high repetition rate (1KHz), the system is also capable of being extended as a time resolved detector for reaction processes. As a future measurement, intense lines could be monitored as a flowing gas is removed from a reaction vessel and pulled though the waveguide. The intensity of that line could be monitored over time as reactants are introduced to have a time resolved kinetics experiment.

Creative solutions and the extendibility of the waveguide and its components offer a versatile low cost solution for bringing modern physical chemistry research inside the classroom and instructional labs.

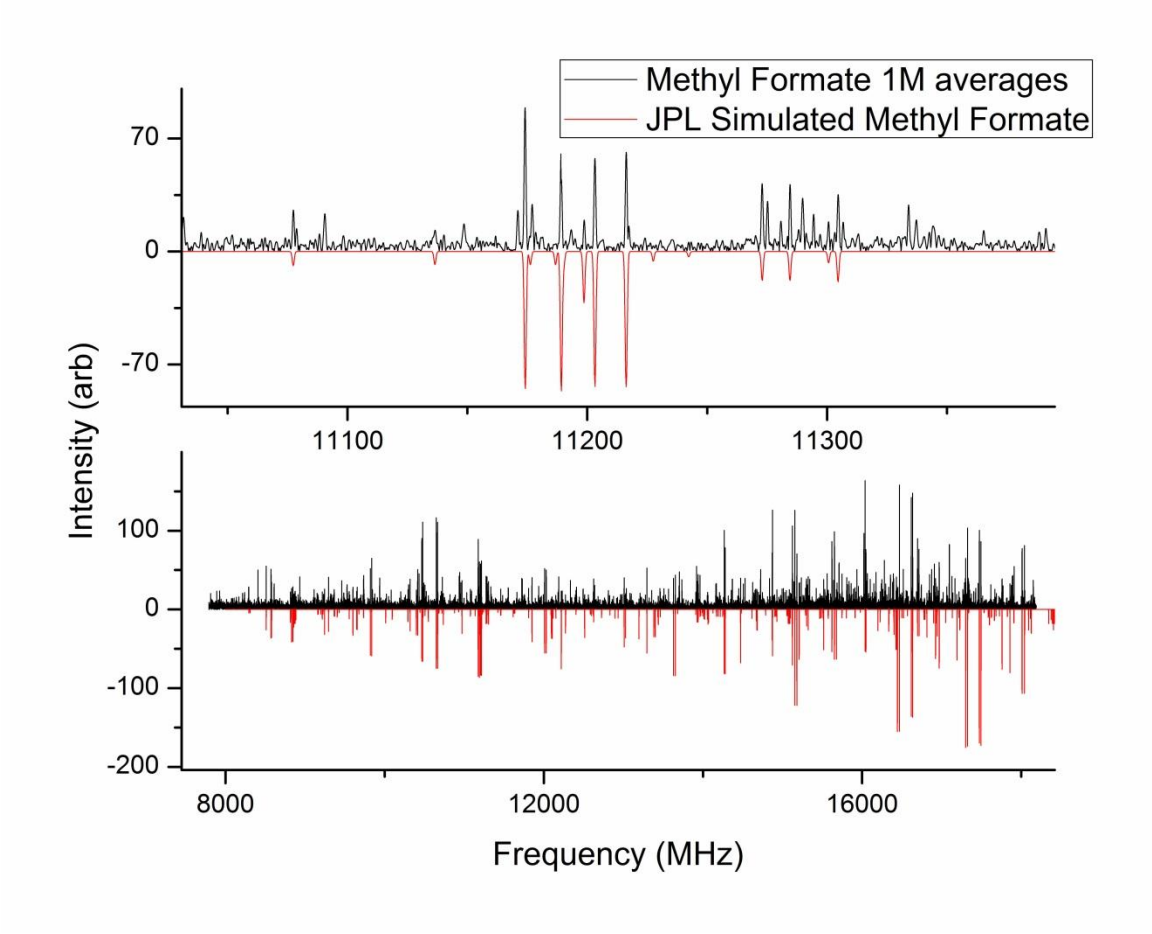

Figure 4: Experimental spectrum of methyl formate at 1M averages (black, positive) plotted against a simulated spectrum from JPL (red, negative). A small frequency range is shown on top to show agreement between predicted and experimental frequencies.

References

[1] McAFEE, K.B.J., HUGHES, R.H., WILSON, E.B.J., 1949. A Stark-effect microwave spectrograph of high sensitivity. The Review of scientific instruments 20.

[2] Robertson, E.G., Godfrey, P.D., McNaughton, D., 2003. The microwave spectrum of o-benzyne measured in a novel Stark modulated spectrometer for transient molecules. J. Mol. Spectrosc. 217, 123–126.

[3] BALLE, T., FLYGARE, W., 1981. FABRY-PEROT CAVITY PULSED FOURIER-TRANSFORM MICROWAVE SPECTROMETER WITH A PULSED NOZZLE PARTICLE SOURCE. Rev. Sci. Instrum. 52, 33–45.

[4] Grabow, J., Palmer, E., McCarthy, M., Thaddeus, P., 2005. Supersonic-jet cryogenic-resonator coaxially oriented beam-resonator arrangement Fourier transform microwave spectrometer. Rev. Sci. Instrum. 76.

[5] Brown, G.G., Dian, B.C., Douglass, K.O., Geyer, S.M., Shipman, S.T., Pate, B.H., 2008. A broadband Fourier transform microwave spectrometer based on chirped pulse excitation. Rev. Sci. Instrum. 79.

[6] Perez, C., Muckle, M.T., Zaleski, D.P., Seifert, N.A., Temelso, B., Shields, G.C., Kisiel, Z., Pate, B.H., 2012. Structures of Cage, Prism, and Book Isomers of Water Hexamer from Broadband Rotational Spectroscopy. Science 336, 897–901.

[7] Hadley, L.N., Dennison, D.M., 1946. The Microwave Spectrum of Ammonia. Phys. Rev. 70, 780–781.

[8] Halpern, A.M., Ramachandran, B.R., Glendening, E.D., 2007. The Inversion Potential of Ammonia: An Intrinsic Reaction Coordinate Calculation for Student Investigation. J. Chem. Educ. 84, 1067.

[9] David, C.W., 1996. IR Vibration-Rotation Spectra of the Ammonia Molecule. J. Chem. Educ. 73, 46.

[10] *H. M. Pickett, R. L. Poynter, E. A. Cohen, M. L. Delitsky, J. C. Pearson, and H. S. P. Muller, "Submillimeter, Millimeter, and Microwave Spectral Line Catalog,"* ***J. Quant. Spectrosc. & Rad. Transfer 60,*** *883-890 (1998).*

Chapter III:

Analytical THz/Sub-millimeter Rotational Spectroscopy

Room temperature mm-wave spectroscopy has existed for many years but until recently existing techniques were often very time consuming especially when acquiring a broadband spectrum. There are a few exceptions such as the FASST[1,2] instrument devolved at Ohio State. The majority of instrumentation available uses a single frequency scanning oscillator slowly working its way across a spectrum in small steps to achieve large bandwidth measurements, have to be frequency calibrated to insure accuracy (unless microwave synthesizers are used as radiation sources), and almost exclusively work by measuring power absorption and thus have to remove the background signal by using double derivative spectra to only look at modulated power changes over narrow ranges[3,4]. These qualities made it so that extending the technique to analytical style measurements would be cumbersome. Specifically, long scan times would lead to inefficient use of measurement times. Because of these long measurement times sample conditions could possibly fluctuate. Additional methods exist involving non-linear optic frequency conversion[16], but those techniques will not be discussed here.

Applying chirped pulse broadband techniques, previously used both at room temperature and pulsed jet, drastically decreases the measurement time while allowing for the use of background free emission measurements. Coupling this drastic increase in measurement speed with this idealized Boltzmann intensity region for room temperature measurements and the fingerprint accuracy of rotational spectroscopy creates the potential for an analytical method for volatile gases that could possibly rival those currently used.

The Experiment

A full detailed description of the instrument can be found detailed in the Journal of Molecular Spectroscopy by Steber *et. al*[13]. The mm-wave instrument vacuum to operate so the chamber is evacuated down to pressures typically below 1mTorr. When the required level is reached, a sample (complex or pure) can be injected via syringe (liquid) or valve (gas/headspace) and fills the sample chamber to a predetermined pressure (2mTorr-100mTorr typical). The sample is held as a static gas and thus only a single aliquot of sample needs to be used (~20μmol typical). This limits sample consumption compared to previous flowing cell methods. The current experimental setup uses a 40L vacuum chamber but ideal solutions would reduce the total volume to match the active microwave region so that sample would not be wasted in non-active regions. Typical volumes needed for a 40L chamber would be ~2ml of gas or ~1-4μL of a typical liquid.

The instrument uses an arbitrary waveform generator to create a chirped light pulse at low microwave frequencies between 2-3.5 GHz at a user defined bandwidth. Because of the frequency agility of the arbitrary waveform generator (Arb) this pulse can be a standard linear frequency sweep covering a set linear bandwidth or a combination of smaller bandwidth pulses that are discontinuous in frequency. The arb can then switch between experimental pulses at real time rates which gives the ability to create a series of small bandwidth pulses that in total, cover a wide frequency range without sacrificing any total measurement bandwidth. In general the smaller bandwidth measurements result in more intense signals, thus the desired sensitivity can be used to determine the measurement bandwidth used. The maximum acceptable bandwidth is set by the digitization rate of the final ADC. For the purposes of this instrument a 4GS real time digitizer was used and the bandwidth was kept under 1GHz to maintain acquisition speed and limit spurious interference (to be discussed in chapter IV). The reduction in bandwidth by a factor of N increases the signal by $\sqrt{N}$, which requires N fewer averages to achieve the same final signal to noise. Thus even though N more measurements have to be made the net time cost is zero assuming the sample is in the weak pulse limit.

The analog light output of the arb is then transferred to a frequency conversion circuit which ultimately creates a mm-wave (260-295 GHz) mm-wave pulse purely from digital electronics. This pulse is passed through a gaseous sample where the molecules are excited to a higher rotational state. The instrument then waits until the power from the initial excitation pulse is out of the sample then collects the background free molecular emission known as the free induction decay (FID). The emitted light is then

down converted through solid state devices to a final frequency between 720-1440 MHz and converted to a digital signal. This signal can then be Fourier transformed to display a frequency spectrum on the output display and later analyzed for composition.

This entire process is completed in 2 microseconds (single line analysis) or 100microseconds (full band analysis) and is repeated/averaged in real time to acquire the final signal. A simplified schematic of the instrument and a process flow chart can be found in Figure 1.

Spectra and Molecular Identity

Using the instrument described above, the rotational spectra of several molecules were measured. As was discussed in an earlier chapter, the measured frequencies are going to be largely dependent on the physical shape and mass of the molecule in question. This allows molecules with the same atomic composition (chemical formula), molecules with similar but not exact shapes, or molecules with similar shapes but different masses (isotopes, different atoms) to give very distinguishable spectra (Figure 2).

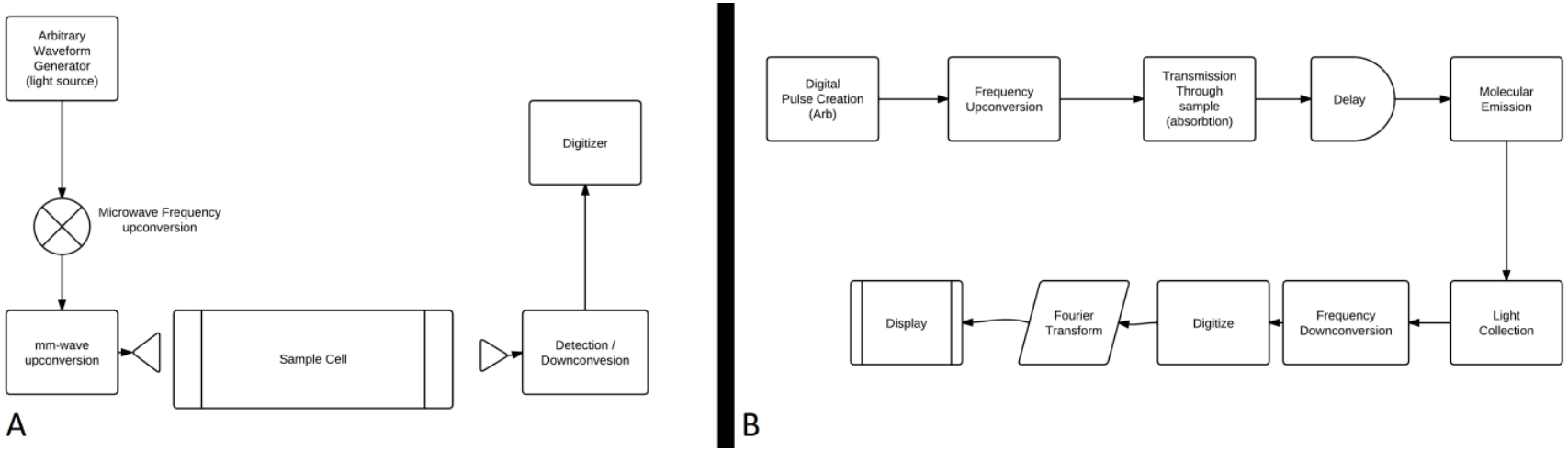

Figure 1: Simplified Schematic (A, left) and Process Flow (B, right) of the mm-wave spectrometer

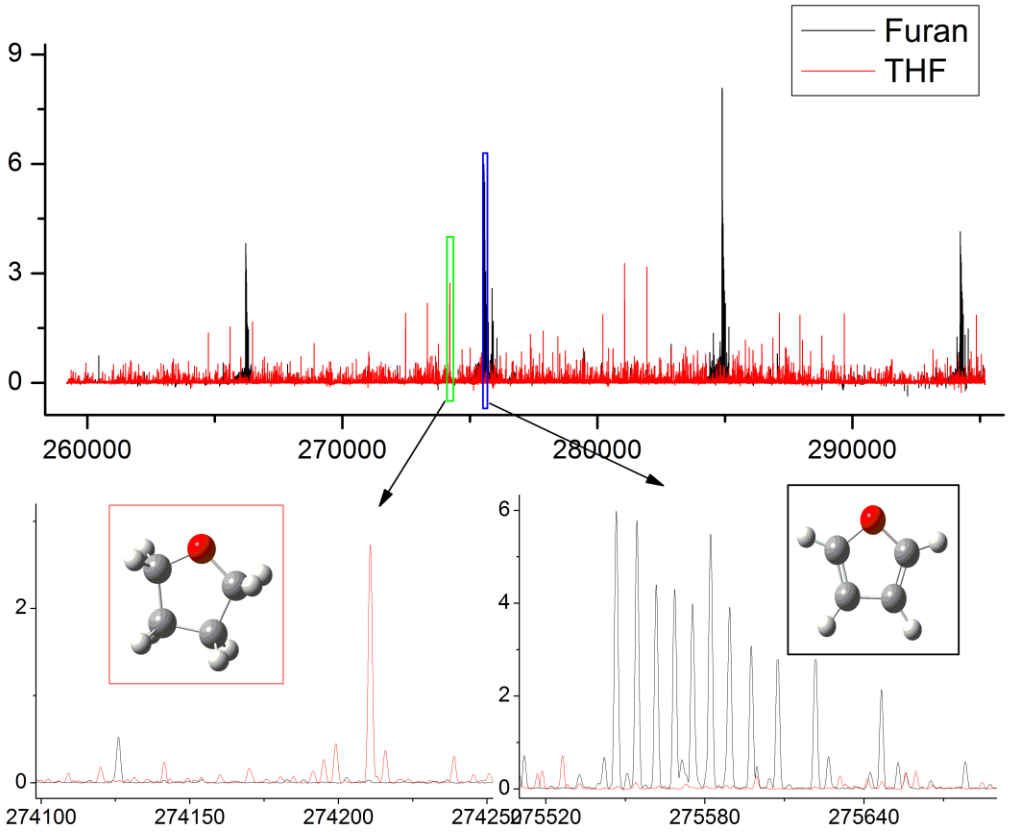

Figure 2: Experimental Spectra of Furan (Black) and tetrahydrofuran(THF, red). Both molecules show similar structure but very visibly distinguishable spectra (top). A zoom on the strongest lines of each(bottom) shows the lack of overlapping lines between the two

Since the spectrum is dependent on the shape of the species, identification of unknown molecules can be made from the assignment of the spectrum. Electronic structure theory is used to calculate a molecules physical shape often to >97% accuracy[14,15]. This structure can produce a calculated spectrum which can be matched with the experimental to identify unknown species.

Another method of deriving a samples identity, involves identifying and fitting the normal species lines and its isotopes in an experimental spectrum to acquire what is known as the substitution structure via Kraitchmans equations[5]. Since small mass changes produce a different spectrum (as discussed in Chapter I), the spectra of a molecule's isotopes, in natural abundance, can be fit in the same experimental spectrum as the parent molecule. The isotopic spectrum (or spectra) appears at intensities scaled down from the normal species by their natural abundance (i.e. 13C~1%, 18O~0.2%).

As an example, the spectrum of Furan (C_4H_4O) was measured using the mm-wave spectrometer using 40,000 averages in 4 seconds. The spectra of the carbon and oxygen isotopomers were then simulated using SPCAT[12] from published constants by Bak *et. al*[6]. The intensities of the simulated spectra are scaled to match their expected natural abundance in Furan (Figure 3) , and one can see that those intensities, to visual approximation, match very well with those in the experimental spectrum. These accurate relative intensities ease the identification of the isotopes which then permits the user to identify the structure of a known molecule or an unknown molecule from a single experiment by

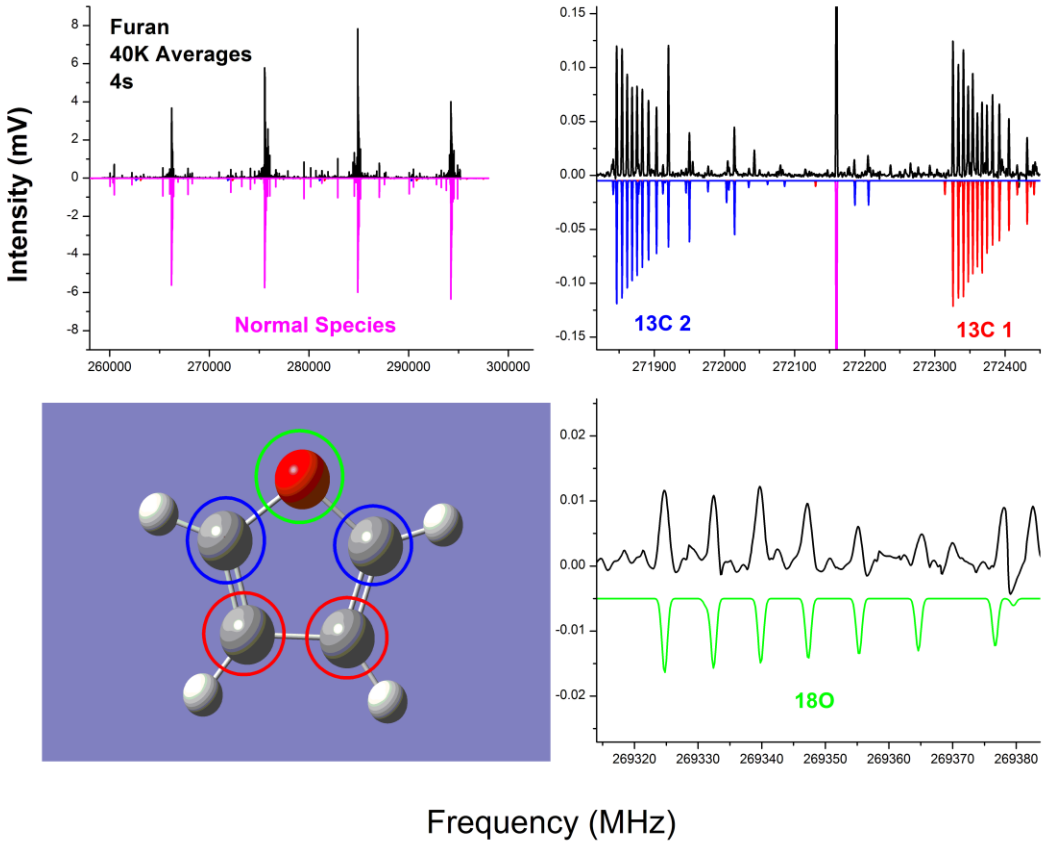

Figure 3: Experimental spectrum of Furan and its carbon and oxygen isotopomers (black, positive) vs simulated spectra from measured constants[6] (colored, negative). Atom positions are circled with their respective color on the molecular structure (bottom left).

limiting the intensity range in which to search for possible isotopomer transitions. Once the spectra of the normal species and isotopologs of an unknown sample are fit one can assume isotopolog mass identities by their relative abundance. These resulting spectra can then be used to calculate the final structure via shifts in the moments of inertia with no previous knowledge of the molecular identity. This unknown species identification tool is an extremely powerful technique to apply to analyzing mixtures or samples of unknown composition as many other standard and common techniques often require the use of an analytical standard or spectral library to confidently identify the compound in question[7].

Sensitivity and Resolution

Beyond qualitatively identifying an unknown species it's important for an analytical instrument to be able to quantitatively determine the abundance in a sample. When trying to measure a complex mixture with many current analytical methods, purification or separation methods, such as chromatography, often have to be applied before measurement to avoid the risk of confusion[8] . The mm-wave instrument instead has linewidths of ~2MHz at baseline allowing over 15000 independent transitions to be measured before there is any blending at the baseline and over 30000 lines to be measured before they start to become unresolvable(where peaks begin to blend) when using the typical 30GHz bandwidth of the instrument.

This high resolution allows complex mixtures to be measured without interference between species. Figure 4 shows two different dense experimental spectra from ϒ-

butyrolactone(GBL) and β-butyrolactone(BPL) that on full scale would seemingly suffer from a large number of overlapping lines convoluting the spectra should they be measured in the same sample. Yet one when looks more closely at a magnified region (the area in green) it can be seen that nearly zero of the transitions from the species overlap leaving large amounts of baseline where there is zero signal between them. Since this is the case, both samples can be measured simultaneously. Even with complex mixtures, one can still distinctly identify each individual molecular species all without the need for any separation.

Eventually in the ultimate limit of complexity, the confusion limit, these lines will begin to blend, but even in that limit identification and quantification is still possible. Often the majority of the lines present are much weaker than the strongest lines in the spectrum and for large species there are often many equal intensity strong lines like in BPL. As long as some of these lines are unconvoluted, an identification can still be made. Additionally quantification is still possible as the intensities of these lines are set by the transition moment of the transition which can be calculated. Simulated spectra can be overlaid and intensities fit algorithmically to extract individual abundances. Similar techniques are applied when analyzing complex astronomical spectra in the radio and far IR[9].

Now that qualitative identifications of multiple species can be made in a single spectrum, one should examine the ability to quantitatively determine the

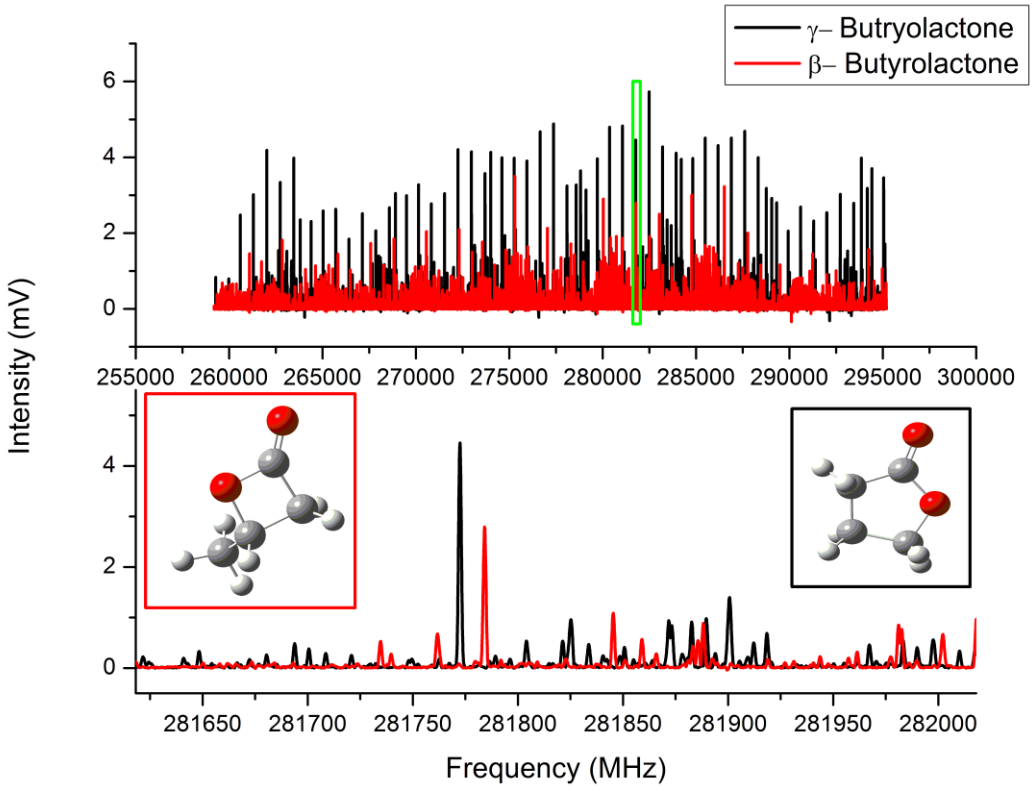

Figure 4: Experimental spectra of ϒ-butyrolactone(Black) and β-butyrolactone (Red) from 260-295GHz overlayed (Top). Very small numbers of overlapping lines are seen when zooming to inspect individual lines(Bottom).

abundances of the measured species. The intensity of the measured spectra is directly proportional to the electric field of the light applied, the number of molecules, and a property of the molecules known as the transition moment (not to be discussed here). The magnitude of the electric field will be the sum of all the electric field of all the emitters (molecules) in the system. Thus the final signal will scale linearly with the total abundance of that species in the system. Then the ability to chirp the pulse, as opposed to transform limited broadband pulses, allows for a stable electric field across a large frequency range giving good relative intensities as can be seen by the relative abundances of the isotopes of Furan in Figure 2. The linear scaling with the number of molecules is demonstrated with the linear scaling of the signal intensity vs. pressure (thus number of molecules) with carbonyl sulfide (OCS)(Figure 5).

Since the intensity of the transition is going to scale linearly with the number of molecules, by either the measurement of some standard at known concentration, or knowledge of the molecular constants (rotational and dipole) one can then calculate the absolute concentrations measured by the instrument. If the molecular constants are known for the species of interest, the standard measured does not need to be of the species of interest but only used to determine the response of the spectrometer to a molecular sample. This then leads to quantifying the sensitivity of the instrument by measuring its detection limits of various sample systems. B measuring the largest signal in the experimental spectrum of various molecules and the average noise level we can extrapolate a detection limit for each species assuming a 3:1 signal to noise ratio needs to be achieved (Table 1). The detection limit will improve with longer measurement time, but for the purposes of practicality in an analytical

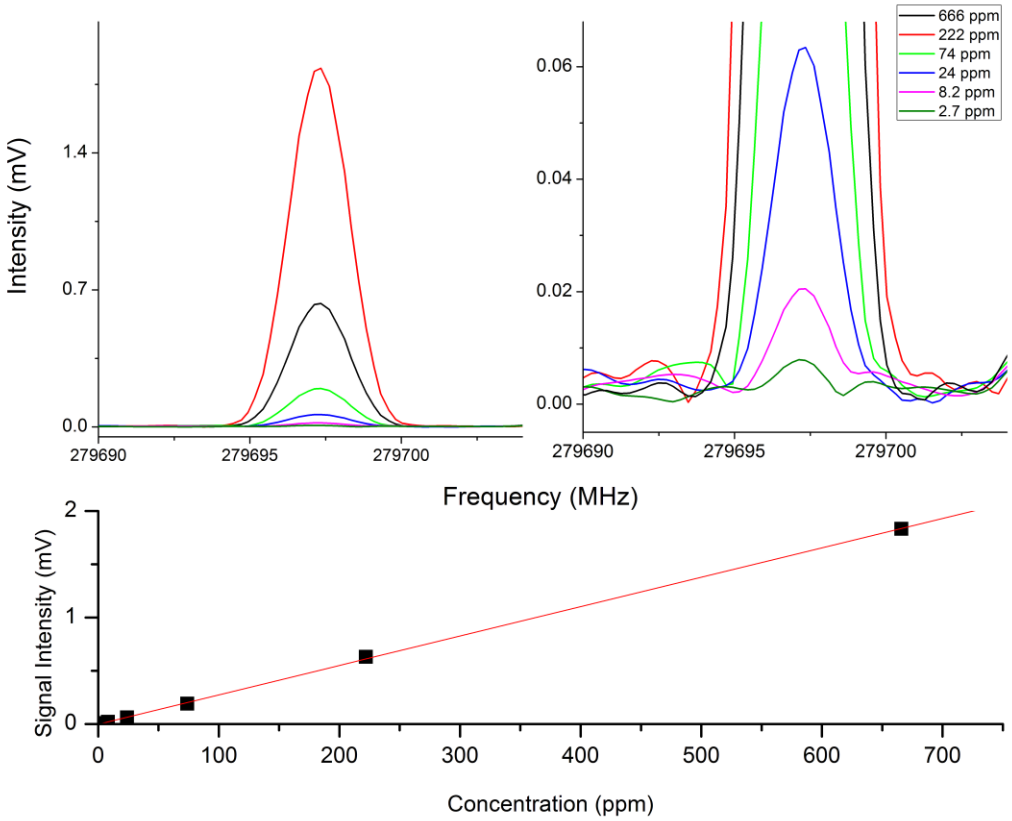

Figure 5: Visual scaling of the signal intensity of J=23-22 of Carbonyl Sulfide (OCS) with pressure (Top). OCS signal vs. concentration in nitrogen (black) fit with a linear regression (red). Sample concentrations are determined by measuring relative pressures using a baratron pressure instrument.

instrument one minute measurements are shown below. These measurements below are a non-exhaustive list, meant to be representative of the potential range of the instrument.

The detection limits shown below (ppb level) are approaching that of cavity ring down (CRDS) and various other laser techniques[10,11]. Yet unlike CDRS where a single instrument is typically designed around detecting a narrow set of species, the mm-wave instrument is capable of detecting a large fraction of polar species in the system at once given its large bandwidth and high resolution. This drastically reduces total measurement time and gives a better assurance to the user of an accurate molecular assignment.

Conclusion

Due the use of high frequency electronics and the emergence of broadband technology rotational spectroscopy is now approaching levels of performance in speed and sensitivity that can compete with current commercial level instrumentation. The speed of the technique allows real-time detection for increased measurement throughput while being able to detect a wide range of molecules simultaneously. It offers a confidence in qualitative detection unrivaled by nearly any other spectroscopic technique as well as accurate quantitative detection into the low parts per billion in only one minute of measurement. With the future addition of algorithmic analysis techniques mm-wave rotational spectroscopy offers a highly sensitive an accurate measurement method with a potential bright future in analytical fields.

Table 1: Detection limits for various molecular species using the mm-wave spectrometer. Ppm/ppb measurements are parts per X in Nitrogen (in molecules). Volumes assume room temperature. ***Liquid volumes not calculated for gas samples. Single line limits are extrapolated from full band measurements. Full Band=FB, Single line=SL

Molecule	FB 1m (ppm)	SL 1m (ppb)	FB 1m (pmol)	SL 1m (pmol)	FB 1m (pL)	SL 1m (fL)
Acetone	10.42	300.85	69.96	2.02	5.14	148.30
B -butyrolactone	2.95	85.19	19.81	0.57	1.62	46.62
B-propiolactone	0.60	17.46	4.06	0.12	0.26	7.37
CPCA	7.38	212.96	49.52	1.43	3.70	106.83
Ethylene Sulfide	0.79	22.69	5.28	0.15	0.31	9.07
G-butyrolactone	1.81	52.31	12.16	0.35	0.81	23.33
Methyl furan	103.28	2981.42	693.35	20.02	61.41	1772.65
Methyl formate	2.79	80.58	18.74	0.54	1.15	33.15
Nitromethane	2.25	64.81	15.07	0.44	0.81	23.36
THF	3.18	91.74	21.33	0.62	1.73	49.94
1-Butyne	36.72	1060.08	246.53	7.12	***	***
OCS	0.47	13.46	3.13	0.09	***	***
Propyne	2.38	68.60	15.95	0.46	***	***
Ethyl Cyanide	1.10	31.70	7.37	0.21	0.53	15.18
Furan	4.52	130.44	30.33	0.88	2.21	63.68
Pyrrole	1.08	31.06	7.22	0.21	0.50	14.47
Methanol	25.01	722.09	223.90	6.46	9.06	261.54

References

[1]Albert, S., De Lucia, F., 2001. Fast Scan Submillimeter Spectroscopy Technique (FASSST): A new analytical tool for the gas phase. Chimia 55, 29–34.

[2]Medvedev, I.R., Behnke, M., De Lucia, F.C., 2006. Chemical analysis in the submillimetre spectral region with a compact solid state system. Analyst 131, 1299–1307.

[3]Ziurys, L.M., Barclay, W.L., Anderson, M.A., Fletcher, D.A., Lamb, J.W., 1994. A millimeter/submillimeter spectrometer for high resolution studies of transient molecules. Review of Scientific Instruments 65, 1517–1522.

[4]Winnewisser, G., Krupnov, A.., Tretyakov, M., Liedtke, M., Lewen, F., Saleck, A., Schieder, R., Shkaev, A., Volokhov, S., 1994. Precision broadband Spectroscopy in the Terahertz Region. Journal of Molecular Spectroscopy 165, 294–300.

[5]Kraitchman, J., 1953. Determination of Molecular Structure from Microwave Spectroscopic Data. American Journal of Physics 21, 17.

[6]Bak, B., Christensen, D., Dixon, W.B., Hansen-Nygaard, L., Andersen, J.R., Schottländer, M., 1962. The complete structure of furan. Journal of Molecular Spectroscopy 9, 124 – 129.

[7] Budde, W. Analytical Mass Spectrometry: Strategies for Environmental and Related Applications. 2001. American Chemical Society. Oxford University Press.

[8]Zlatkis, A., Bertsch, W., Lichtenstein, H.A., Tishbee, A., Shunbo, F., Liebich, H.M., Coscia, A.M., Fleischer, N., 1973. Profile of volatile metabolites in urine by gas chromatography-mass spectrometry. Anal. Chem. 45, 763–767.

[9]Medvedev, I.R., De Lucia, F.C., 2007. An experimental approach to the prediction of complete millimeter and submillimeter spectra at astrophysical temperatures: Applications to confusion-limited astrophysical observations. Astrophys. J. 656, 621–628.

[10]Abe, H., Yamada, K.M.T., 2011. Performance evaluation of a trace-moisture analyzer based on cavity ring-down spectroscopy: Direct comparison with the NMIJ trace-moisture standard. Sensors and Actuators A: Physical 165, 230–238.

[11]Wojtas, J., Bielecki, Z., Stacewicz, T., Mikolajczyk, J., Nowakowski, M., 2012. Ultrasensitive laser spectroscopy for breath analysis. Opto-Electron. Rev. 20, 26–39.

[12] H. M. Pickett, "The Fitting and Prediction of Vibration-Rotation Spectra with Spin Interactions," J. Molec. Spectroscopy 148**,** 371-377 (1991)

[13] Steber AL, Harris BJ, Neill JL, and Pate BH. An Arbitrary Waveform Generator Based Chirped Pulse Fourier Transform Spectrometer
Operating from 260-295 GHz. J. Mol. Spec. (accepted 2012).

[14] Shipman, S.T., Neil, J.L., Suenram, R.D., Muckle, M.T., Pate, B.H., 2011. Structure Determination of Strawberry Aldehyde by Broadband Microwave Spectroscopy: Conformational Stabilization by Dispersive Interactions. J. Phys. Chem. Lett. 2, 443–448.

[15] Perez, C., Muckle, M.T., Zaleski, D.P., Seifert, N.A., Temelso, B., Shields, G.C., Kisiel, Z., Pate, B.H., 2012. Structures of Cage, Prism, and Book Isomers of Water Hexamer from Broadband Rotational Spectroscopy. Science 336, 897–901.

[16] Han, P.Y., Zhang, X.-C., 2001. Free-space coherent broadband terahertz time-domain spectroscopy. Measurement Science and Technology 12, 1747–1756.

Chapter IV:

Limits in Dynamic Range

When constructing a spectrometer it is very useful to be able to have an idea on the instrument's limits. One of the important limits that one has to take into mind is the instrument's its total dynamic range. Can one measure and average a signal infinitely or is there some limit beyond which additional measurements then become useless?

When examining a broadband rotational spectrum, the transitions that have been identified and fit can be removed to only look at the residual spectrum. Figure 1 shows such a residual spectrum from Suprane (desflurane). This residual spectrum appears remarkably dense and thus it is difficult to pick out the same visual patterns used to fit high signal to noise spectra. Even when one zooms to only look at a small portion of the spectrum the baseline appears to be a near continuous wall of transitions. This begs one to question if these are actual molecular transitions or some artificial noise floor that is limiting the dynamic range of the experiment.

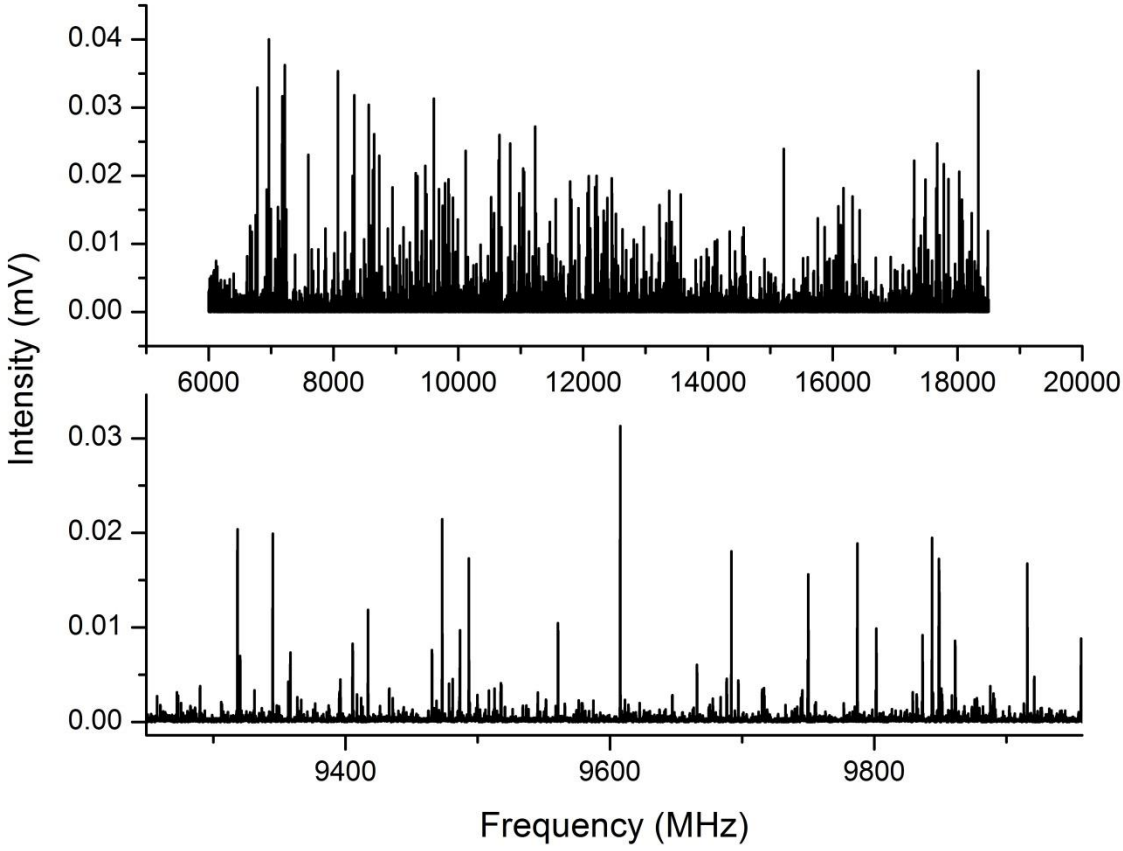

Figure 1: Residual spectrum of the 6-18 direct detection CP-FTMW measurement of Suprane (top) taken at 0psi backing pressure (gague). A zoom of a small window on the full band spectrum is shown to display spectral density on the bottom.

In the case of a broadband Fourier Transform microwave spectrometer[1], one is continuously averaging molecular emission in the form of a sine wave oscillating around zero. Since only phase coherent signals locked to the measurement timescale will average, one could imagine in the limit of an infinite number of averages the amplitude of the recorded signal should approach zero in the case of no molecular emission. This would then give a system where the ultimate detection limits of the instrument would also be infinite, even though the suprane spectrum mentioned earlier seems to hint at the start of a noise floor limit.

The first exception to this rule would be the recording hardware and software's ability to store the signal values in a digital number. This limit can easily be circumvented with various software methods and large storage devices but is there is an additional hardware limit before this would even have to be considered.

When measuring the broadband spectrum, a series of solid state digital devices must be used. These digital devices suffer from two main problems, spectral purity[2] and non-linear responses[3]. For these cases, we will ignore electronics used in the excitation half of the FTMW and look solely at the effects in the detection level as these two halves should be sufficiently isolated from one another. These non linear responses and spectral purity issues can lead to spurious signals (spurs) of non-molecular origin that may limit the ultimate dynamic range of the experiment. These spurs are common issues tackled when dealing with the design of high speed digital electronics often used in communications[3,4]. A similar problem is seen and accounted for in the digitizers used for

FT-IR spectroscopy[5]. These spurs are dubbed intermodulation distortion products since they are generated through the intermodulation of two, or more, input tones into a device. These spurs and their effect on the final molecular spectrum acquired through broadband rotational spectroscopy and solutions to reduce their final impact will be discussed.

Non-linear responses

Ideally high frequency electronic device such as cables, amplifiers, and digitizers, should behave with a linear response (frequency 1 in = only frequency 1 out) unless specifically designed to behave elsewise (mixers, multipliers, etc). Unfortunately, most devices will still exhibit some small non linear response[3,4] even in the simplest of components (cables, amplifiers, connectors, filters, etc). These non linear responses effectively result in mixing of the input waves, where the output of the devices now emits sum and difference frequencies at combinations of the input. These outputs can then create "ghost" signals the can eventually create an artificial noise floor in the finial digitization limiting the dynamic range of the instrument. The product frequencies are known as intermodulation spurs.

These output signals can be referenced by their "order." The first order/fundamental would be the original input signal, second order are products of two wave mixing (harmonics, sum/difference frequencies) and third order exist as a sum/difference product of a fundamental and a second order product. Each of these output waves can be calculated by the Taylor series below where E_n is the amplitude of the electric field, ν_n is the input frequency, and C_{xy} is the transfer function for the

efficiency of the mixing of the input waves x,y. An example of these mixing results is shown in Figure 2.

$E_1*\cos(2*pi*\nu_1*t) + E_2*\cos(2*pi*\nu_2*t) +$ **(fundamental)**

$C_{12}*E1*\cos(2*pi*\nu_1*t) * E_2*\cos(2*pi*\nu_2*t) +$ **(2^{nd} O. Difference/Sum)**

$C_{11}*E1*\cos(2*pi*\nu_1*t) * E_1*\cos(2*pi*\nu_1*t) +$ **(Harmonic ν_1)**

$C_{22}*E2*\cos(2*pi*\nu_2*t) * E_2*\cos(2*pi*\nu_2*t) +$ **(Harmonic ν_2)**

$C_{122}*E1*\cos(2*pi*\nu_1*t) * E_2*\cos(2*pi*\nu_2*t) * E_2*\cos(2*pi*\nu_2*t) +$ **(3^{rd} O. off ν_2)**

$C_{112}*E1*\cos(2*pi*\nu_1*t) * E_2*\cos(2*pi*\nu_2*t) * E_1*\cos(2*pi*\nu_1*t)$ **(3^{rd} O. off ν_3)**

Here the largest focus lies with the third order mixing spurs as they will often fall in the same measurement band as the fundamental and thus cannot easily be filtered. This is because these 3^{rd} order products are only separated from their parent transitions by the beat frequency of the parents which is often less than 1-2GHz between strong lines. The 2^{nd} order spurs instead are often only 1-2GHz for their lower side band and far above the measurement bandwidth for the upper sideband (aliasing is still a possibility, but this is usually prevented through filtering). The majority of the harmonics as well ($2\nu_x$) will also fall above

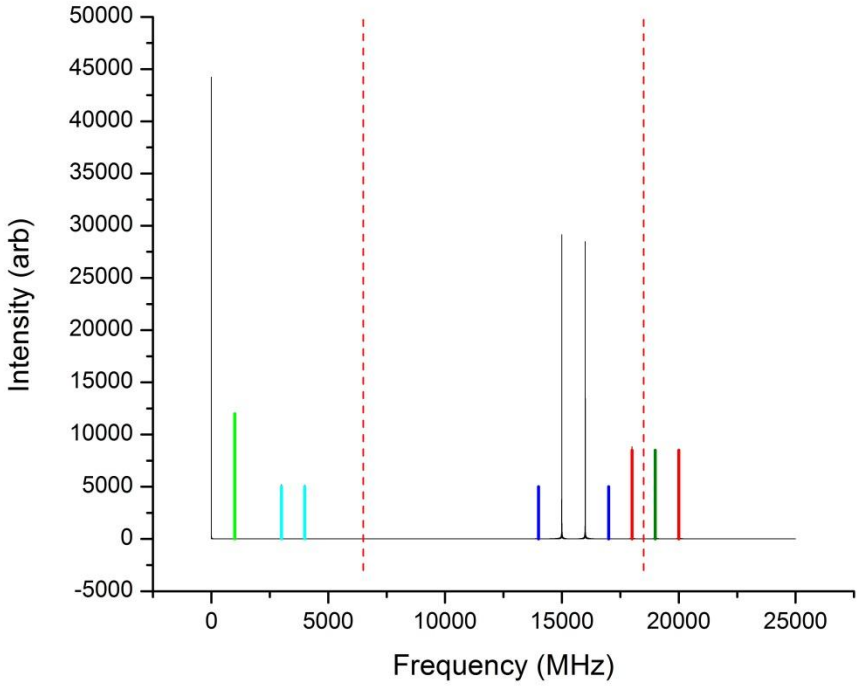

Figure 2: Calculated non-linear mixing spectrum from two equal intensity fundamentals (15,16GHz) for a 50GS/s system. Fundamentals are shown in black, second order in light green, second order (aliased) red/dark-green, third order blue, third order (aliased) light blue. The measurement band lies between dashed red lines.

the measurement band, except in the instances where ν_{max}, the maximum frequency in the measurement bandwidth is greater than $\nu_{mix,}$ the minimum frequency in the measurement bandwidth. For a typical 6.5-18 GHz measurement only transitions at 6.5- 9GHz will have the possibility to exhibit harmonics in the final spectrum. Higher order mixing products are possible but are not discussed here.

The number of third-order spurs scales with the number of potential mixing waves (N^3) and thus these third orders can be very numerous within the bandwidth of the measurement and can quickly convolute the final data by creating a multitude of false transitions around baseline. The harmonics and second order spurs will only fall in the measurement band under certain conditions and experimental setups, are less numerous than the 3rd order spurs but can be more intense. This leads the potential to create ghost transitions that could confuse the experimentalist when fitting experimental spectra or, in the ultimate limit, creates an artificial noise floor limiting the dynamic range of the final instrument. Thus since the 3rd order will be the primary contributor to the spur density within the experimental bandwidth, if the experiment is primarily in the second Nyquist zone (the upper half of the digitizer limit), the ability to predict and control these spurs eases the ability to get large dynamic range measurements without hitting line confusion from artificial signals.

Predictions

As mentioned above, the positions of the non-linear mixing spurs can be calculated by using simple cosine wave products to result in a sum and difference resultant frequency. A simulated spectrum of the resulting calculation is shown in Figure

2. The efficiency parameters, C, in a normal experiment is often <<<1, but were set as 1 for easy viewing in the simulated spectrum. The vertical red dashed lines surround the typical measurement bandwidth of one operating band of a CP-FTMW spectrometer (6.5-18.5 GHz). The only lines within the measurement bandwidth are the two fundamentals (at 15 and 16 GHz, in black), two of the 3 rd order mixing spurs (dark blue), and the alias of the second harmonic of the 16 GHz transition. In an actual experiment the aliased transitions are normally significantly weaker due to hardware filtering by natural low pass filtering of system components. Thus the majority of spurs that fall into the measurement region from non-linear mixing of molecular transitions will be the 3rd order products.

The intensities of these 3 rd order products will scale with the product of the electric field of the three constituent mixing waves. The spur intensity will then drop by $\sqrt{8}$ when the input signal (Electric field) drops by $\sqrt{2}$ (Figure 3). This expedited scaling allows one to picture the resulting effect on various spectral scenarios. First, only the most intense lines will mix and create the strongest spurs due to the relative signal: spur intensity ratio scaling. Intense sparse spectra will thus suffer from strong spurs but the majority of the data channels in a spectrum will be unaffected. A dense, intense fundamental spectrum will suffer from intense spurs as well, but with the added problem of having many spurs that

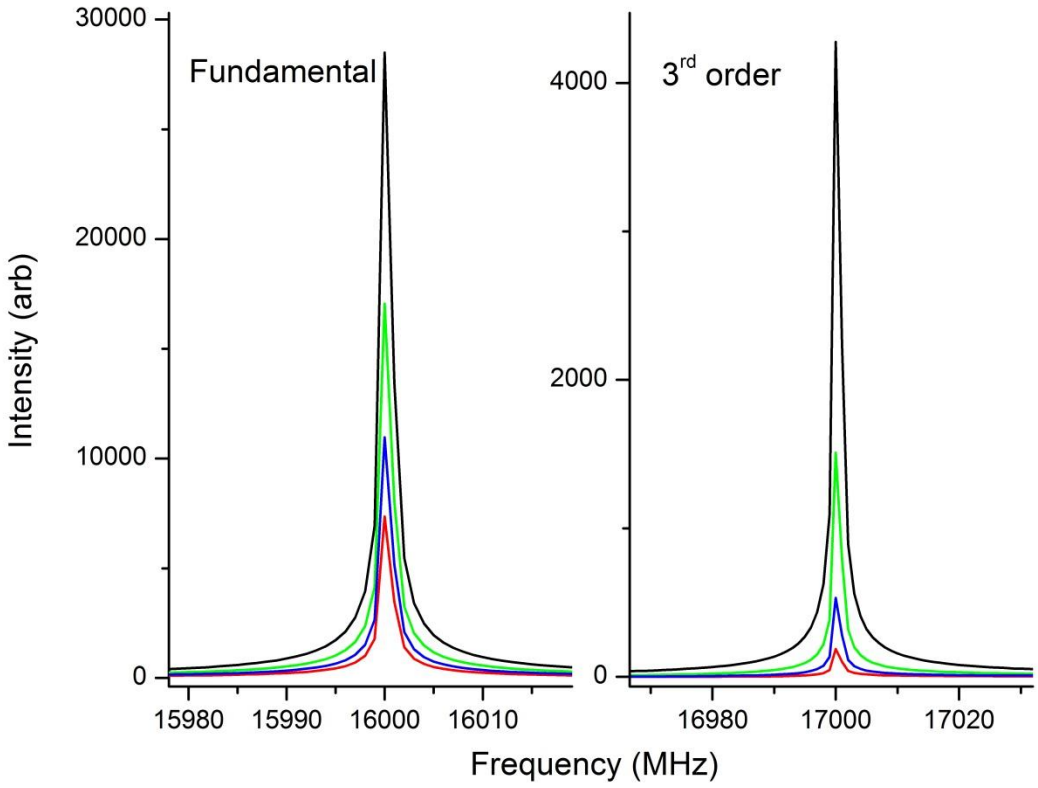

Figure 3: Theoretical spur scaling: Left: Intensity reduction by $\sqrt{2}$ of the fundamental transition results in a $\sqrt{8}$ reduction in the intensity of the 3 rd order spur intensity (right).

can eventually create an artificial baseline confusion limit. Finally, weak spectra, dense or sparse, will not efficiently mix and will only exhibit very weak spurs that will allow for a larger dynamic range before hitting the confusion limit. Thus, if one could attenuate the input signal to the non-linear device without adversely affecting signal to noise, one could drastically reduce the intensity of spurs and thus increase the potential dynamic range.

Experiment

The theoretical existence of these 3 rd order spurs was first verified by measuring the spectrum of methyl formate with the 6-18 GHz CP-FTMW. Methyl formate has a single pair of strong transitions (A and E state) in the middle of the operating band of the instrument (12.219 GHz) separated by approximately 1 MHz. These two lines result in two 3 rd order spurs located offset to the molecular transitions by the splitting of the two molecular lines (~1 MHz) at an intensity of 1/60th the fundamental transition as seen in Figure 4. The spectrum was then reacquired 4 times while varying the attenuation after the low noise amplifier directly before entering the oscilloscope at steps of 3dB from 10-19dB. The attenuation range was chosen to keep the signal on one digitizer scale (10mV/division) of the oscilloscope to avoid rescaling the internal variable amplifier before the digitizer. The resulting normal molecular species lines were scaled to equal intensity between attenuations and the top panel of Figure 4 then shows the reduction in relative spur intensity from the attenuation of the input signal as predicted by the theoretical cosine wave mixing.

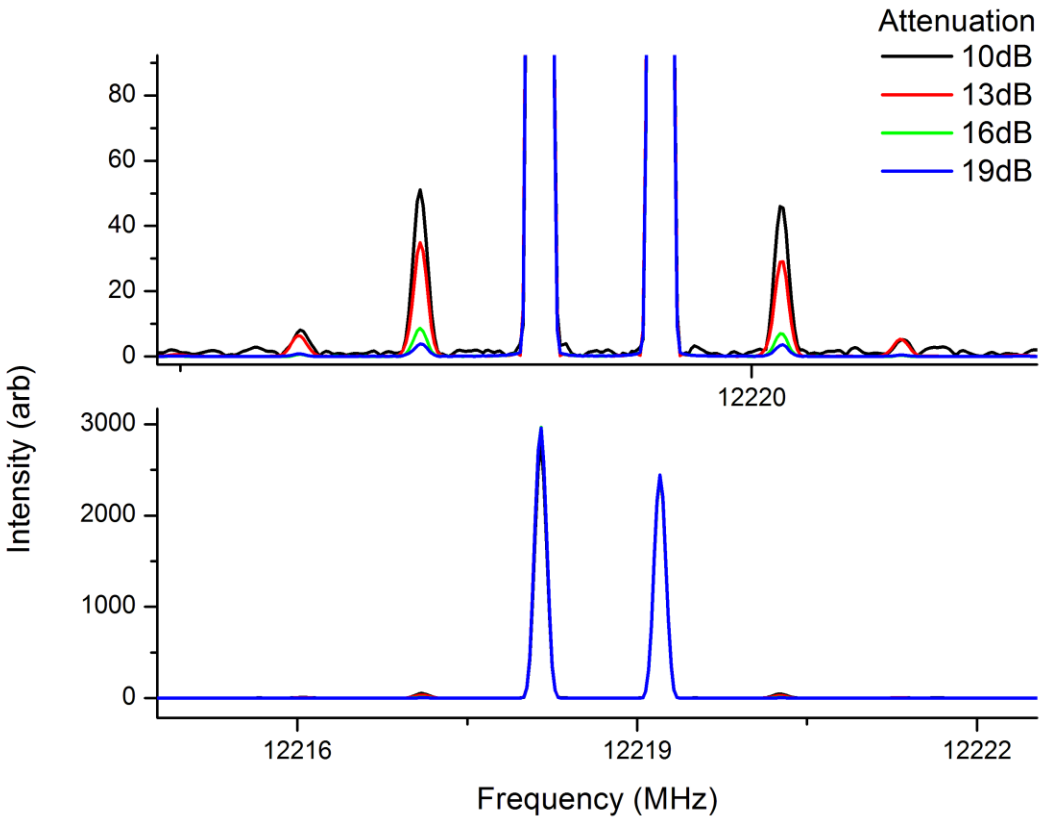

Figure 4: Experimental spectrum of methyl formate. (Bottom) Normal species A, E states of the 1_{01}-0_{00} transition at various input attenuations scaled to the same ultimate signal level. (Top) Zoom showing reduction in 3rd order spur intensity relative to the normal species line with greater attenuation.

Identifying Spurs in Dense Spectra

As previously mentioned, the sparse spectra will result in few but intense intermodulation spurs but the dense spectra from large molecules can result in a carpet of weaker spurs that can limit the dynamic range of the measurement. The ability to predict and remove these spurs from a measurement would greatly enhance the ability to fit the remaining molecular transitions by removing misleading lines. Additionally, understanding the relative intensity of the spurs allows for advanced planning for effective use of measurement time as to understand the practical dynamic range of a measurement.

Suprane (desflurane) was used as a benchmark large dense and intense molecule. The full spectrum acquired between 6-18 GHz can be seen in Figure 5 for an idea of spectral density. The absolute molecular signal is roughly an order of magnitude weaker than the aforementioned methyl formate signal meaning the largest spurs should be >1000x weaker than the molecular transitions in the case of Suprane.

The direct calculations of the cosine mixing of two waves was rather calculation intensive because of the need to create a full 1 million point artificial FID so using the same method as used to simulate the spurs earlier, to calculate the mixing products of a dense spectrum like Suprane would be computationally long and inefficient. Instead a line list of the experimental spectrum was generated using peak picking algorithms and then only the lines with intensities >50% of the strongest transition were fed into a second algorithm. All combinations of the beat frequencies

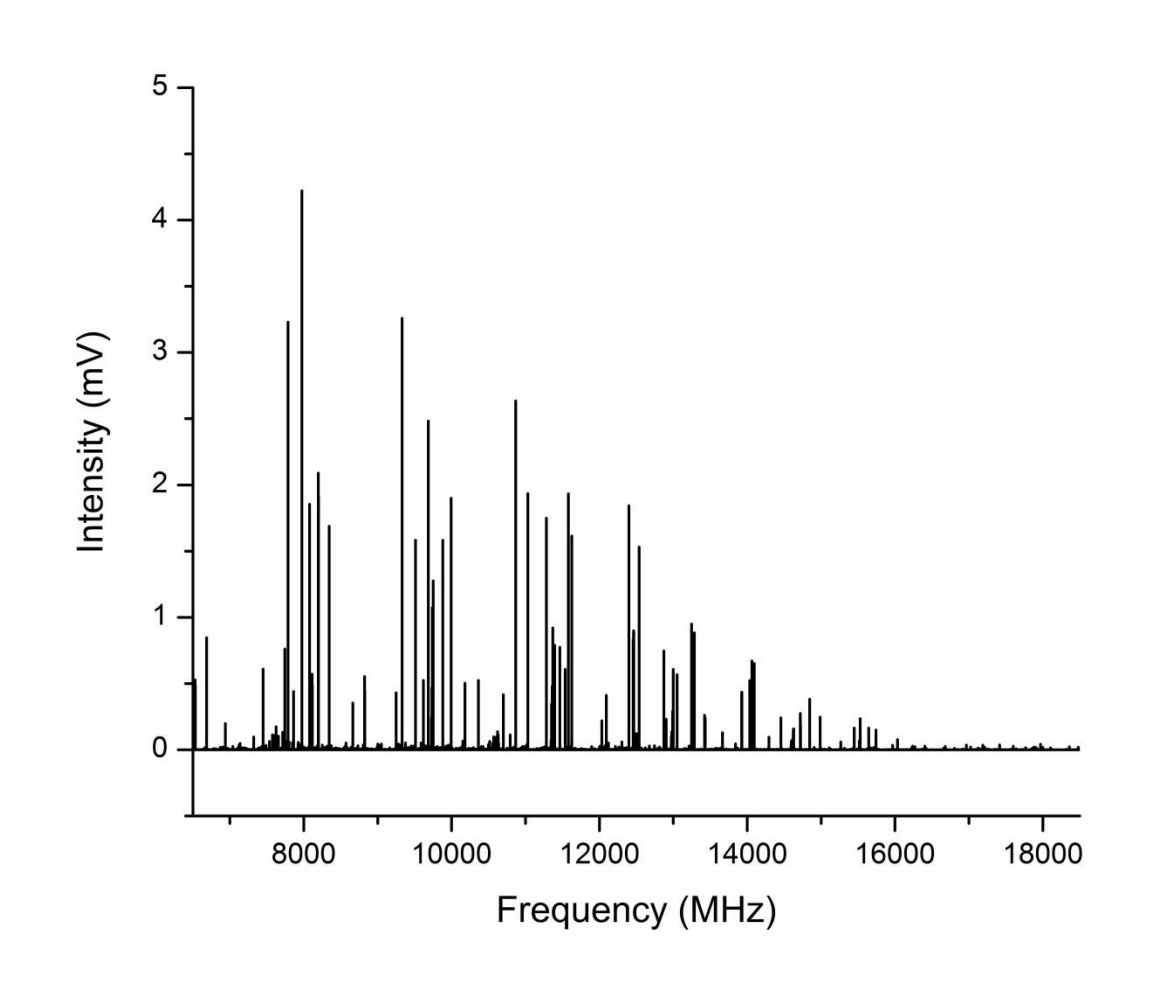

Figure 5: Experimental chirped pulse direct detection spectrum of suprane at 1M average with an excitation ranging from 6.5-18.5 GHz.

(lower side band of 2nd order mixing) of these lines were then calculated with their intensities as the product of the intensities of the fundamentals. These beat products were then filtered to only allow lines >50% the strongest beat through. Finally the 3rd order spurs were calculated by subtracting and adding every allowed beat frequency to every filtered fundamental with their intensities as the product of the intensity of the beat with the intensity of the fundamental. The resulting line list of potential spurs was used to simulate a full spectrum with Gaussian line shapes as seen in Figure 6. The simulated lines were scaled to a single matching ghost transition in the experimental spectrum. The resulting overlap between the experimental and prediction accounts for many of the transitions near the baseline with good relative intensity agreement. These spurious lines appear at approximately 3000 down from the normal species molecular lines near the assumed value of ~1000 as scaled from signal to spur ratio seen with methyl formate.

The relative intensity of the spurs was reduced in methyl formate by attenuating the input signal to the oscilloscope so the same experiment was repeated with Suprane in a hope to remove many of the spurs experimentally without having to cut the lines algorithmically. Algorithmic cutting would be frowned upon as it would remove data channels from the experiment. This is because these spurs are effectively using up data channels that could otherwise be occupied by low abundance isotopes, weak conformers, or weakly bound species. Unfortunately, current methods of predicting the intensity of these spurs are not accurate enough to warrant direct background subtraction to preserve the data channels.

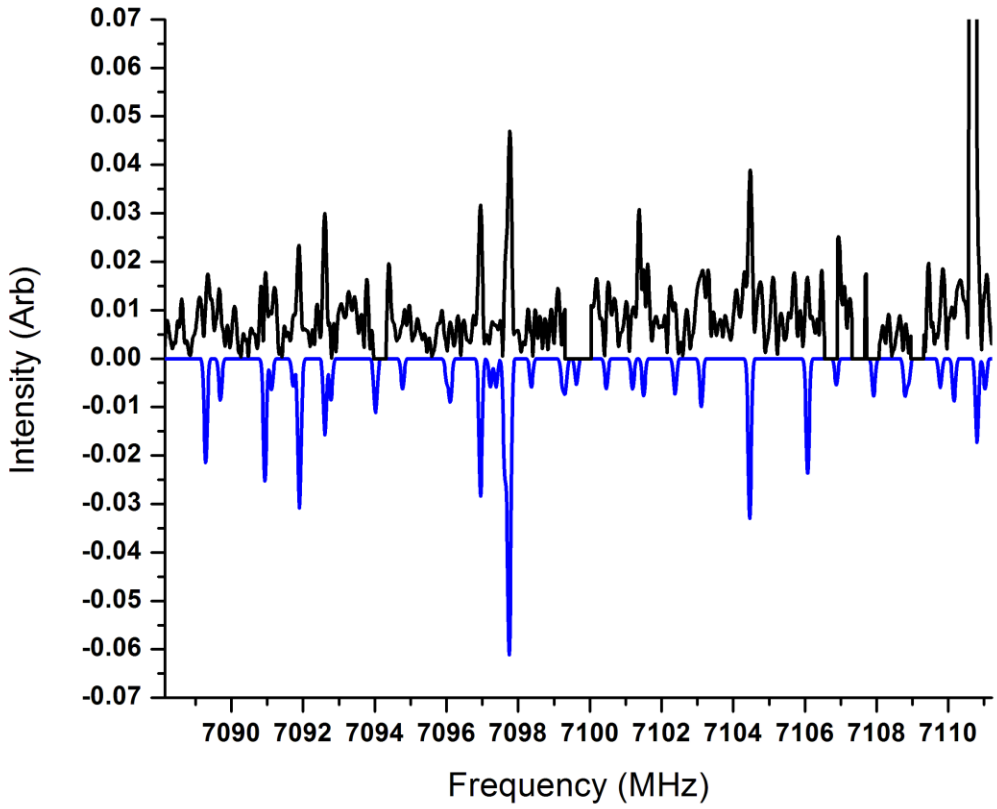

Figure 6: Section of the experimental spectrum of Suprane (black positive) with a simulated spectrum of calculated spurs (blue negative).

The same suprane measurement was repeated with 6 dB of attenuation in front of the oscilloscope reducing the input power by a factor of 4 and, ideally, the spur intensity by a factor of 8. This would reduce even the largest spur to below the noise level of the experiment. Figure 7 shows the resulting attenuated spectrum in black with the previous attenuated spectrum in red and the calculated spurs offset in blue. The two experimental spectra were scaled so that the intensities of the normal species lines would match and thus appear at the same signal to noise despite the attenuation. The largest calculated spur indicated by an arrow can be seen in the red but is absent in the black spectrum indicating again that attenuation the input signal will reduce the relative spur intensity and thus increase the effective potential dynamic range of a measurement.

Further Decreasing Spurs

Attenuation, while effective, has its limits and may not be a cure all for eliminating spurs from a measurement. One can only attenuate to a point where the signal is still filling a bit on the measurement digitizer. Any lower and signals will no longer properly fill the digitizer bits and signal to noise will suffer as bit/digitizer noise can dominate over the detection amplifier. In these cases additional measures can be taken.

Only spurs that originate with molecular lines and fall within the measurement bandwidth will contribute to the artificial noise floor and convolute the fitting/analysis and thus anything outside can be easily discarded. Therefore,

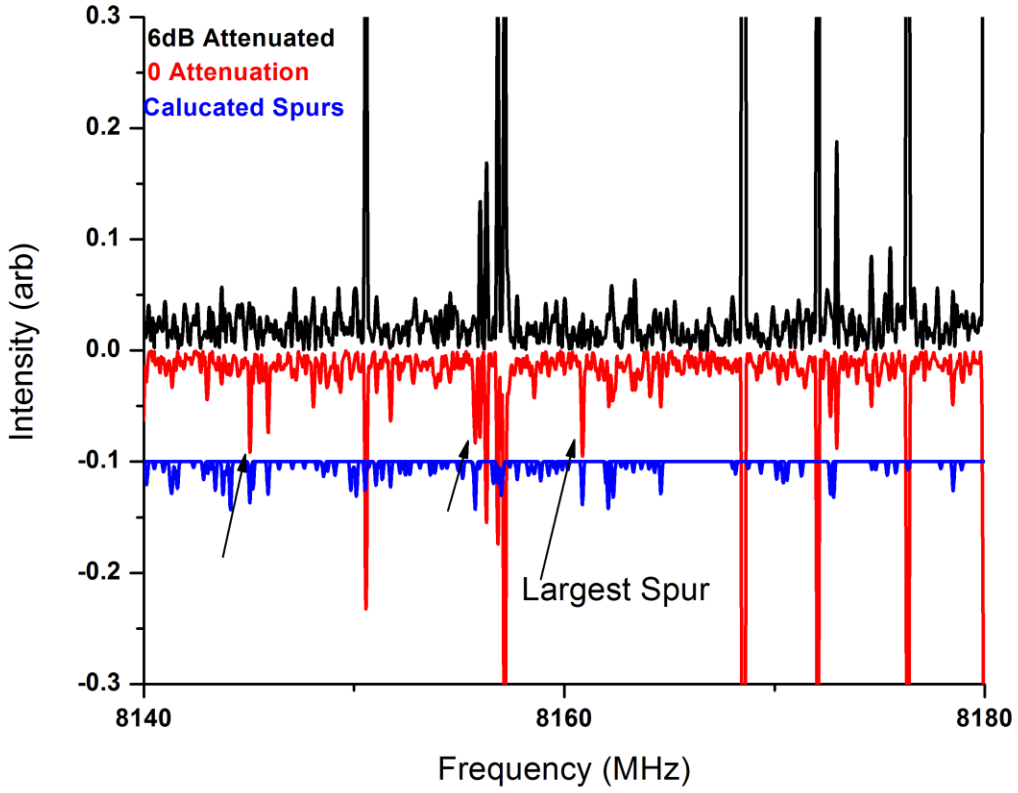

Figure 7: Experimental spectrum of suprane (red, negative) with no attenuation overlaid with calculated spurs (blue) and an attenuated experimental spectrum (black) showing the reduction in spur intensity with attenuation. The largest calculated spurs are marked with arrows.

reducing the bandwidth of the measurement can limit the number of intermodulation lines and thus minimize the number of spurs that can land within the bandwidth of the

measurement. For this example, we will assume a new measurement bandwidth of 1GHz reduced from ~11 GHz previously. While it is true then that the measurement has to be repeated 11 times not at 11 different windows the total time of the measurement is conserved if the transitions are not power saturated. In this weak-field case, a reduction of 11 in bandwidth will increase the signal level by $\sqrt{11}$, thus requiring a factor of 11 reduction in the number of averages (and therefore measurement time) needed to reach equivalent sensitivity, netting even in total measurement time. The downside is because the spur intensity scales with the power in, the relative spur intensity will increase since the signal level is increasing. The intensity of these remaining spurs can then be reduced by the aforementioned attenuation of the input signal.

Suprane was again selected as a benchmark molecule but only a single spectrum ranging between 8100 and 9100 MHz was acquired with no attenuation at the same 50GS/sec and direct detection as the full band spectrum. The resulting spectrum can be seen in Figure 8 overlaid with the calculated spurs. The overall spur intensity has increased relative to the full band spectrum but the overall density has decreased. A comparison of the theoretical spur density in this region can be found in Figure 9 where the total density reduction with bandwidth reduction becomes very apparent.

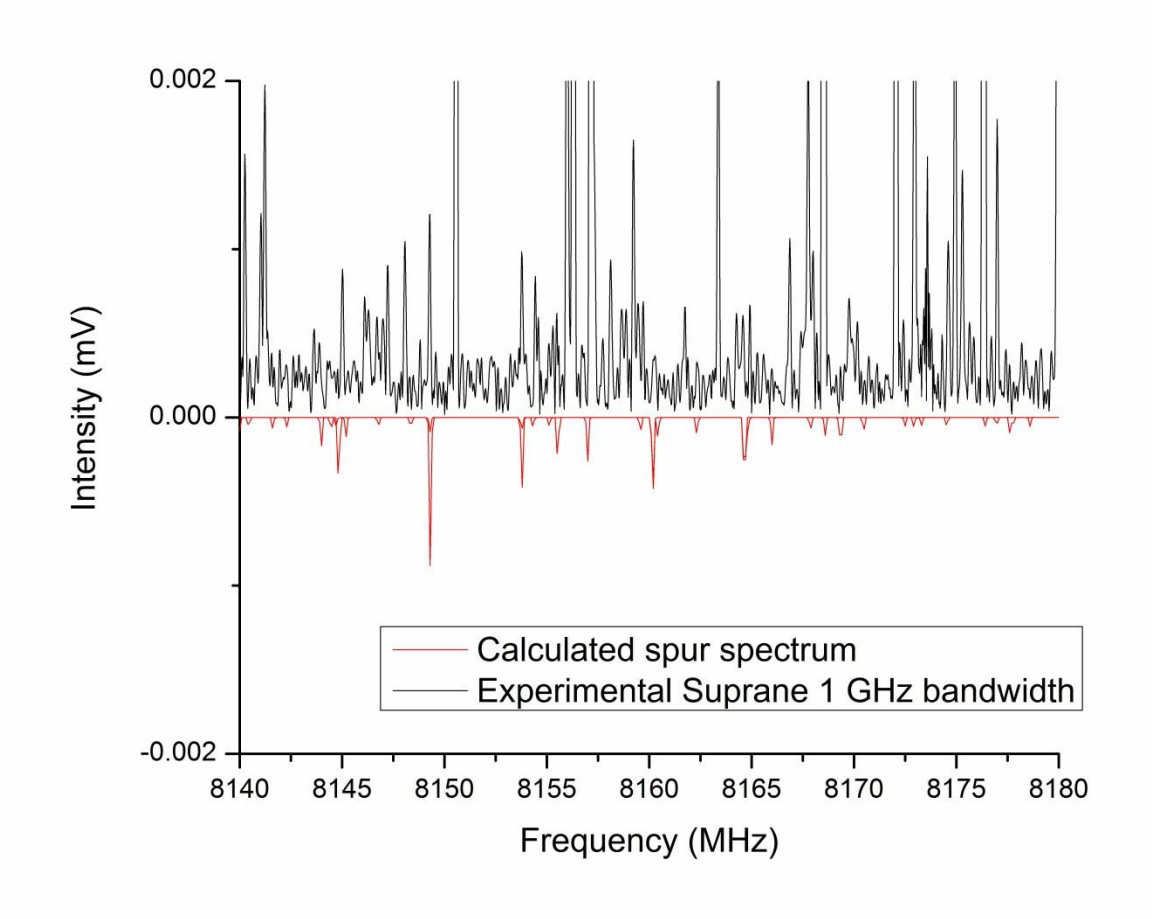

Figure 8: Selection of the experimental spectrum of suprane at a reduced excitation bandwidth of 1GHz (black, positive) showing the low spur density (red, negative) from the reduced number of intermodulating transitions.

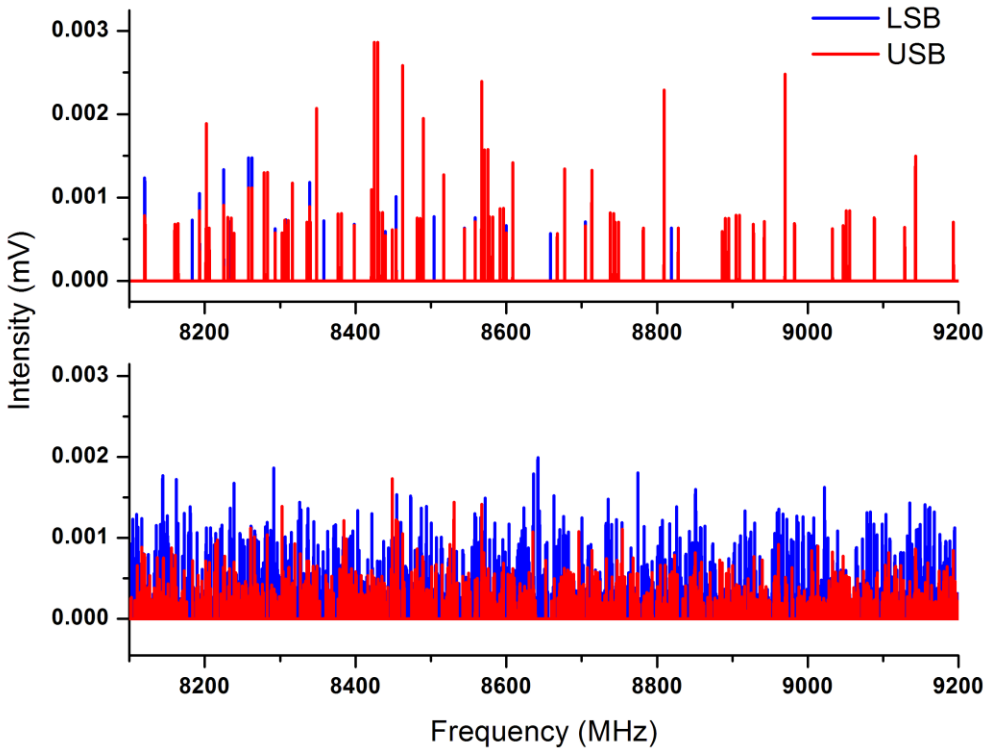

Figure 9: Calculated spurs for suprane at 1GHz reduced bandwidth (top) and full bandwidth (bottom) showing a reduction in spur density with a reduction in bandwidth. Both lower(blue) and upper (red) sidebands (LSB,USB) of the mixing products are plotted separately.

Since this segmentation reduces the total number of potential spurs it can be effectively coupled with attenuation methods discussed earlier to yield the maximum improvement in total sensitivity and purity possible.

Spectral Purity

The molecular emission should be a pure summation of sine waves corresponding to the transition frequencies of the sample, but the electronics along the path to the final digitization can add additional signals to the final detection beyond direct IMD products of only the molecular transitions. In the case of a frequency down conversion detection these spurs can occur both from spectral impurities in the local oscillator (LO) and clock frequencies localized to the digitizer, but a direct frequency detection system should only suffer from the latter of the two. Thus while the direct detection system is preferred for the highest signal purity, frequency converted systems are often required to increase speed or due to technological limitations in digitizer technology.

If the system is using a LO to down convert the signal, often that LO emits weak spurious signals around the intended frequency. Each of these additional frequencies can operate as separate LO's creating multiple image spectra that will be summed into the final spectrum. In the case of a single frequency LO this is often dealt with using a cavity filter to select a single frequency but some newer systems are requiring a fast switching LO generated by an arbitrary waveform generator[6]. These systems cannot be easily filtered and can only be improved by an extremely spectrally pure source, which have only just recently reached the market.

In the case of digitizer clock line generated spurs, digitizers use a base processor clock to sync the acquisition of the signal. Since these clocks are directly connected to the acquisition chips, their frequencies and harmonics can leak through to the final detection. Fortunately these are often suppressed and are also sparse, as compared to molecular lines and 3rd order intermodulation spurs, and won't raise the noise floor[7]. For example the Tektronix oscilloscope, currently in use with the UVA chirped pulse instrument, uses a base 3.125GHz clock thus spurs appear at 3.125GHz, 6.25GHz, 12.5GHz, and 25GHz when using the 50GS/sec digitizer setting. While not numerous, these clock lines can be subjected to the non linear effects by intermodulating with molecular transition frequencies.

The same non linear responses discussed previously can then cause these clock lines to mix with the molecular signal and cause an image of the molecular spectrum to appear. Ideally the manufacturer of the digitizer attempts to minimize the intensity of these clock lines through calibration methods but this calibration is not always 100% effective. Figure 10 denotes a particularly bad, but non-typical, example of clock mixing with suprane. The top panel shows the normal species suprane spectrum, while the bottom shows the residual spectrum where the frequency axis of the full uncut spectrum was inverted and scaled to match the normal species spectrum. These types of mixing effects pose a real problem as their density can quickly begin to swamp low intensity signals and

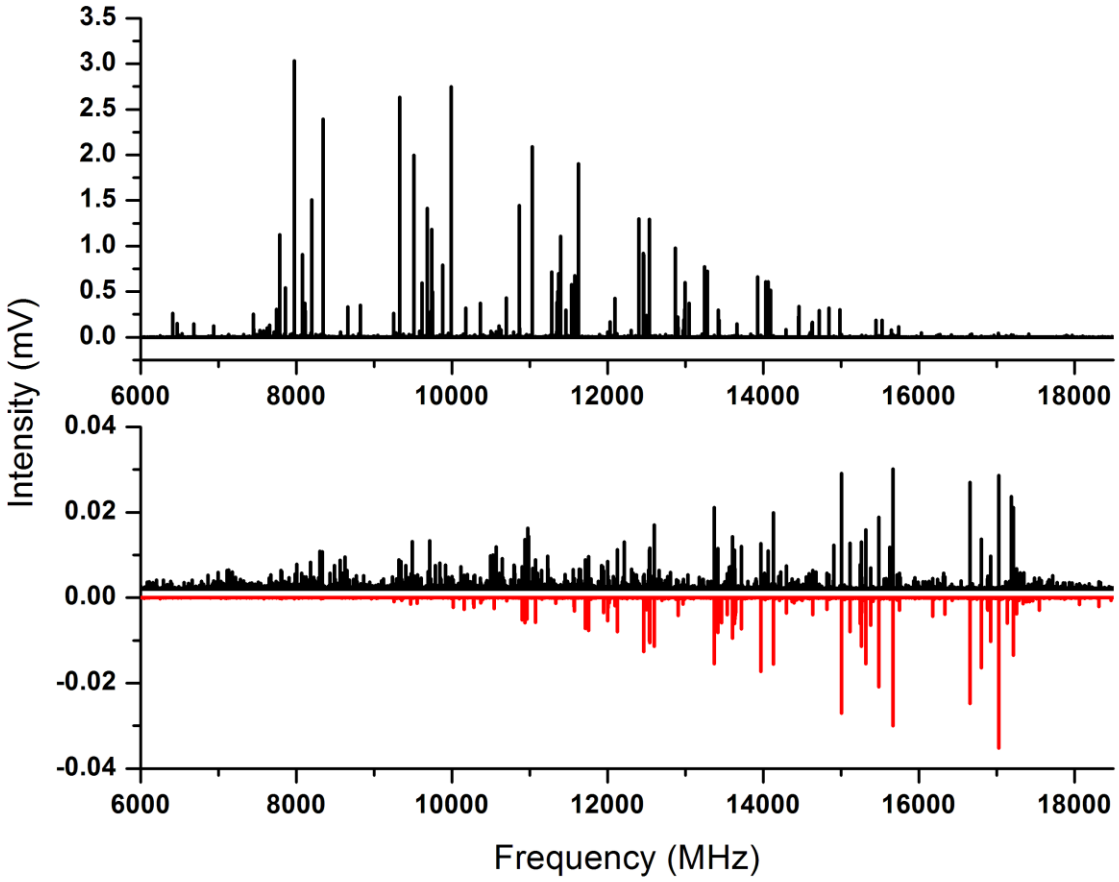

Figure 10: Experimental normal species spectrum of Suprane (top). (Bottom) The residual spectrum of Suprane (positive, black) overlaid with a scaled uncut spectrum of Suprane with an inverted frequency axis(red, negative) showing an image spectrum for mixing with a 25GHz clock spur.

remove a large portion of the data channels available. Outside of fixes and calibration by the manufacturer, no real experimental method has been proposed to decrease their effect on the spectrum.

Conclusion

The ability to measure high dynamic range spectra for low abundance species in large bandwidths is a prized ability of broadband rotational spectroscopy, but the limit of the ability has never been known. The same digitizer that allows the technology to flourish also has the ability to create some of its ultimate limitations through spurious signals. These signals have the potential to create a confusion limited baseline through artificial signals. Yet with the ability to manipulate the input power to the scope with simple attenuation methods coupled to more advanced bandwidth reductions has the potential to extend the practical operating range.

Finally the spectra discussed here were some of the worst case scenarios. As demonstrated, the direct detect measurements require a very intense signals to create problematic spurs and those spectra also have to be very dense in order to create confusion limited noise floors through intermodulation mixing. These dense fundamental spectra often do not have the same strong intensity of suprane so they are often much less of a problem. Yet it is possible with future improvements to the technique these intensities could rise and the number of samples requiring attention to these intermodulation spurs will rise dramatically.

References

[1]Brown, Gordon G., Brian C. Dian, Kevin O. Douglass, Scott M. Geyer, Steven T. Shipman, and Brooks H. Pate. "A Broadband Fourier Transform Microwave Spectrometer Based on Chirped Pulse Excitation." *Review of Scientific Instruments* 79, no. 5 (May 2008).

[2]Rabijns, D., Van Moer, W., Vandersteen, G., 2004. Spectrally pure excitation signals: Only a dream? IEEE Trans. Instrum. Meas. 53, 1433–1440.

[3]Kim, S., Elkis, R., Peckerar, M., 2009. Device Verification Testing of High-Speed Analog-to-Digital Converters in Satellite Communication Systems. IEEE Trans. Instrum. Meas. 58, 270–280.

[4]Remillard, S.K., Yi, H.R., Abdelmonem, A., 2003. Three-tone intermodulation distortion generated by superconducting bandpass filters. IEEE Trans. Appl. Supercond. 13, 3797–3802.

[5]Baghdadi, A., Gladden, W.K., Flach, D.R., 1986. Nonlinear Effects of Digitizer Errors in FT-IR Spectroscopy. Applied Spectroscopy 40, 617–628.

[6] Steber AL, Harris BJ, Neill JL, and Pate BH. An Arbitrary Waveform Generator Based Chirped Pulse Fourier Transform Spectrometer
Operating from 260-295 GHz. J. Mol. Spec. (accepted 2012).

[7] Kuo, C.-Y., Chang, J.-Y., Liu, S.-I., 2006. A spur-reduction technique for a 5-GHz frequency synthesizer. IEEE Transactions on Circuits and Systems I: Regular Papers 53, 526 –533.